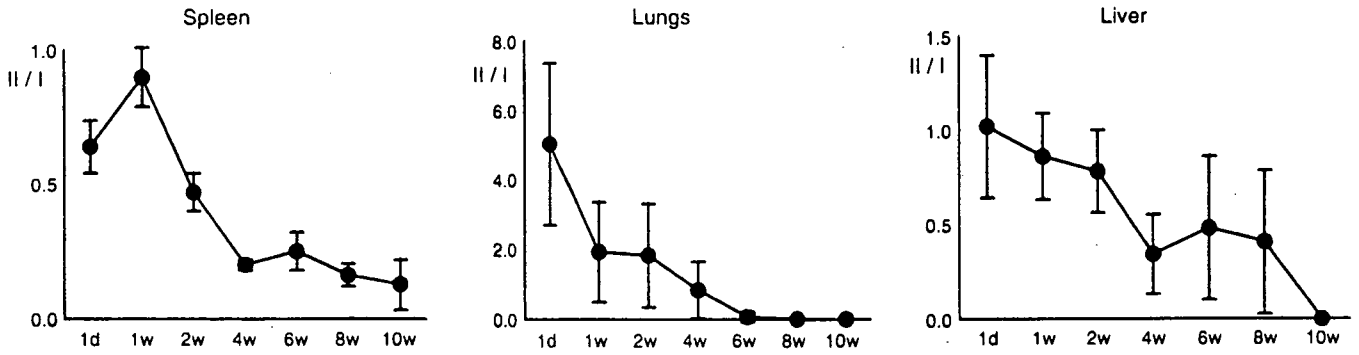

Fig. 6. Competition experiment in mice organs showing a growth advantage of type I over type II. A mixture of equal amounts of type I and type II (10 μg wet weight, 3.1×10^5 CFU) was intravenously injected into C57BL/6 mice ($n = 5$), and the changes of the type II/type I ratio in the spleen, lungs and liver from 1 day to 10 weeks after injection were investigated. Type II/type I ratio was estimated from the recovered CFU numbers having S- or R-colony morphology. Error bars: standard deviations.

R-colony morphology) in the spleen, lungs and liver showed a tendency to decrease over time in every case (Fig. 6).

4. Discussion

In BCG Tokyo172 substrain, the two colony morphologies (smooth: S and rough: R) were strongly related to the two genotypes, i.e., type I with a 22 bp deletion in *Rv3405c* of RD16, and type II without the deletion, similar to many other BCG substrains. As far as we know, this is the first time that a relationship between colony morphology and genotype in BCG has been identified. Type II likely corresponds to the genotype which Bedwell et al observed, and speculated might involve contamination of BCG Tokyo with another substrain [5]. Since they also found that this genotype had an identical multiplex PCR pattern to that of BCG Birkhaug, we conducted experiments to determine if type II is different from BCG Birkhaug or not. As a result, it was newly found that type II gave different results from BCG Birkhaug on DU2 in tandem duplication analysis. This is the first time in which tandem duplications were analyzed and compared between BCG substrains by PCR, and the results suggested a possibility for distinguishing BCG substrains by this method. IS6110 RFLP of types I and II produced two bands (unpublished data), similar to the results reported for Tokyo172 [10], while the Birkhaug substrain is known to show a single band [11]. Accordingly, type II was considered to be genetically different from BCG Birkhaug. Type II was present in every Tokyo172 preparation studied including the seed lot, the origin of seed lot, and ATCC BCG Japan. Also, the RD regions (including RD16) and SenX3-RegX3 of types I and II were stable after 20 serial passages in three types of media (same as those used in growth competition experiment, data not shown), indicating that transition from type II to type I is unlikely. Altogether, it was suggested that types I and II represented different genotypes, each constituting different subpopulations within the Tokyo172 substrain, and that this was not caused by the contamination of another BCG substrain. Since the proportion of type II seemed lower in ATCC BCG Japan than in other Tokyo172 preparations, and the sensitivity of multiplex PCR for minor components is not high, it is not surprising that Bedwell et al. could not find a type without the 22 bp deletion in RD16 region (type II) in ATCC BCG Japan.

An association between colony morphology and RD16 genotype was implied in this study, which raises the possibility of using colony morphology as a substitute for RD16 genotyping of Tokyo172 preparations. The morphology of BCG colonies is suggested to be related to cell wall components such as mycoside B [12], and a deletion in *Rv3405c*, which codes for a possible transcriptional regulatory protein (Tuberculist, http://genolist.pasteur.fr/TubercuList/) of which the function is not yet clear, might affect their synthesis or metabolism through some ways. However, rare exceptions did exist, i.e., some R-colonies had a type I genotype, and some S-colonies had a type II genotype. This might indicate the existence of factors other than the deletion in *Rv3405c* of RD16, which influence colony morphology. It is not clear if these exceptions are distinct genotypes within types I or II, or caused by changes in the expressions of some genes outside *Rv3405c*. The fact that BCG Moreau, which has a complete deletion of RD16, showed a rough colony morphology similar to type II when grown on 7H10 medium (data not shown) also suggests the existence of more complicated mechanisms.

In every Tokyo172 preparation studied, S-colonies exceeded 90% of the total. Accordingly, it is probable that the Tokyo172 preparation is mainly comprised of type I genotype, and that the known characteristics of this preparation, such as high viability and good heat stability [13], are those of type I bacilli. Type I probably arose from type II by mutation after delivery of BCG to Japan in 1924, since a similar deletion in RD16 has not been found in other BCG substrains so far [5,9]. From its relative abundance, type I is considered to correspond to the 'spreading colonies' which Osborn have reported [4] (and probably type II corresponds to the 'non-spreading colonies'), but difference in colony spread was not apparent on Middlebrook 7H10 agar. Type I seemed to have

growth advantage over type II both on culture media and in mice organs, and the former in vitro tendency might be one of the reasons why type I was always the major component of the Tokyo172 preparations. Judging from the present results, the 22 bp deletion in *Rv3405c* did not seem to affect growth in vitro or in vivo. It is not known if this deletion does not affect the growth of type I because *Rv3405c* is not expressed/functional, or if there exists some unknown difference between the genotypes of types I and II, which compensates for the drawback of this deletion and further favors growth of type I. Preliminary experiments have indicated that immunogenicity, which is believed to be related to the replication of BCG in the host [13], also seemed to be greater for type I than type II, as determined from IFN-γ secretion by sensitized spleen cells (data not shown). However, early preferential accumulation of type II (at 1 day) in the lungs (and also to some extent in liver) was observed, although it was cleared rapidly thereafter. The reason for this, and whether this has any consequences on the host responses, are not clear. Deletion in *Rv3405c* might be influencing on this phenomenon, through some changes in surface molecules of the bacilli. In the clinical setting, multiplex PCR investigation of specimens from patients receiving BCG vaccination or BCG therapy for bladder cancer have shown that only the genotype with deletion in RD16 (type I) was recovered in every case [9], results which coincide with the present competition study in mice. These results together with the suggested lower virulence of type II from histopathological studies run in parallel (data not shown), indicate that co-existence of a small amount of type II in the Tokyo172 preparation is unlikely to be problematic by affecting its immunogenicity and safety, although further investigations including protection against virulent *M. tuberculosis* or growth in immunocompromised animals, still need to be continued.

Tokyo172 (BCG Japan) is known to be one of the three substrains (Japan, Moreau, and Russia) with the fewest genetic mutations [8]. Among them, Japan had smallest deletion [14], and this remains true even when the 22 bp deletion of RD16 is included. Moreover, the type II bacilli of Tokyo172 (lacking the deletion in RD16) might be one of the BCG which most inherited the genotypes of the Calmette and Guérin's original BCG.

Since BCG was not established as a clone, it might be natural that BCG originally consisted of multiple subpopulations with different genotypes, and this characteristic is still maintained by many established BCG substrains including Tokyo172. The same investigations for other BCG substrains will undoubtedly benefit to ensure the safety and reliability of BCG as a tuberculosis vaccine or a therapeutic agent for bladder cancer.

References

[1] Petroff SA, Branch A, Steenken Jr W. A study of bacillus Calmette-Guérin (BCG). I. Biological characteristics, cultural "dissociation" and animal experimentation. Am Rev Tuberc 1929;19:9–46.

[2] Behner DM. The stability of the colony morphology and pathogenicity of BCG. Am Rev Tuberc 1935;31:174–202.

[3] Pierce CH, Dubos RJ. Differential characteristics in vitro and in vivo of several substrains of BCG. II. Morphologic characteristics in vitro and in vivo. Am Rev Tuberc Pulm Dis 1956;74(5):667–82.

[4] Osborn TW. BCG vaccine: an investigation of colony morphology from four different strains after their introduction as seed for vaccine preparation in four production laboratories. J Biol Stand 1983;11:19–27.

[5] Bedwell J, Kairo SK, Behr MA, Bygraves JA. Identification of substrains of BCG vaccine using multiplex PCR. Vaccine 2001;19:2146–51.

[6] Behr MA, Wilson MA, Gill WP, Salamon H, Schoolnik GK, Rane S, et al. Comparative genomics of BCG vaccines by whole-genome DNA microarray. Science 1999;284:1520–3.

[7] Brosch R, Gordon SV, Buchrieser C, Pym AS, Garnier T, Cole ST. Comparative genomics uncovers large tandem chromosomal duplications in *Mycobacterium bovis* BCG Pasteur. Yeast 2000;17:111–23.

[8] Behr MA. Comparative genomics of BCG vaccines. Tuberculosis 2001;81:165–8.

[9] Seki M, Sato A, Honda I, Yamazaki T, Yano I, Koyama A, et al. Modified multiplex PCR for identification of Bacillus Calmette-Guérin substrain Tokyo among clinical isolates. Vaccine 2005;23:3099–102.

[10] Fomukong NG, Dale JW, Osborn TW, Grange JM. Use of gene probes based on the insertion sequence IS986 to differentiate between BCG vaccine strains. J Appl Bacteriol 1992;72:126–33.

[11] Behr MA. BCG-different strains, different vaccines? Lancet Infect Dis 2002;2:86–92.

[12] Abou-Zeid C, Rook GAW, Minnikin DE, Parlett JH, Osborn TW, Grange JM. Effect of the method of preparation of Bacille Calmette-Guérin (BCG) vaccine on the properties of four daughter strains. J Appl Bacteriol 1987;63:449–53.

[13] Gheorghiu M, Lagrange PH. Viability, heat stability and immunogenicity of four BCG vaccines prepared from four different BCG strains. Ann Immunol (Inst Pasteur) 1983;134C:125–47.

[14] Mostowy S, Tsolaki AG, Small PM, Behr MA. The in vitro evolution of BCG vaccines. Vaccine 2003;21:4270–4.

Available online at www.sciencedirect.com
SCIENCE DIRECT
ELSEVIER
Microbial Pathogenesis 40 (2006) 245–253
MICROBIAL PATHOGENESIS
www.elsevier.com/locate/micpath

Mycobacterial sulfolipid shows a virulence by inhibiting cord factor induced granuloma formation and TNF-α release

Yuko Okamoto [a], Yukiko Fujita [a,*], Takashi Naka [a], Manabu Hirai [b], Ikuko Tomiyasu [c], Ikuya Yano [a]

[a] *Japan BCG Central Laboratory, 3-1-5 Matsuyama, Kiyose-shi, Tokyo 204-0022, Japan*
[b] *Osaka City University Medical School, 1-4-3 Asahi-machi, Abeno-ku, Osaka 545-8586, Japan*
[c] *Tezukayama University, 7-1-1 Tezukayama, Nara-shi, Nara 631-8501, Japan*

Received 18 October 2005; accepted 10 February 2006
Available online 19 April 2006

Abstract

Virulence mechanism of infection with *Mycobacterium tuberculosis* is currently focused to be clarified in the context of cell surface lipid molecule. Comparing two mycobacterial glycolipids, we observed toxicity and prominent granulomatogenic activity of trehalose 6,6′-dimycolate (TDM) injection in mice, evident by delayed body weight gain and histological observations, whereas 2,3,6,6′-tetraacyl trehalose 2′-sulfate (SL) was non-toxic and non-granulomatogenic. Likewise, TDM but not SL caused temporarily, but marked increase of lung indices, indicative of massive granuloma formation. Interestingly, co-administration of TDM and SL prevented these symptoms distinctively and SL inhibited TDM-induced release of tumor necrosis factor alpha (TNF-α) in a dose-dependent manner. Histological findings and organ index changes also showed marked inhibition of TDM induced granuloma formation by co-administration of SL. Simultaneous injection of SL together with TDM was highly effective for this protection, as neither injection 1 h before nor after TDM injection showed highly inhibitory. In parallel studies on a cellular level, TDM elicited strong TNF-α release from alveolar but not from peritoneal macrophages in vitro. This effect was blocked when alveolar macrophages were incubated in wells simultaneously coated with TDM and SL, indicating that SL suppresses TDM-induced TNF-α release from macrophages. Our results suggest a novel mechanism by which SL could contribute to virulence at early stage of mycobacterial infection or stimulation with the glycolipids by counteracting the immunopotentiating effect of TDM.

Keywords: *Mycobacterium tuberculosis*; Trehalose dimycolate; Cord factor; Sulfolipid; Tumor necrosis factor alpha; Granuloma formation

1. Introduction

Cord factor (trehalose 6,6′-dimycolate, TDM) and sulfolipid (2,3,6,6′-tetraacyl trehalose 2′-sulfate, SL; Sulfatide-1, SL-1) are well-known glycolipids of *Mycobacterium tuberculosis* [1–3], as shown in Fig. 1. Thin-layer chromatographic analysis of glycolipids for *M. tuberculosis* Aoyama B showed two distinctive spots corresponding to TDM and SL (Fig. 2). Both glycolipids, SL and TDM possess trehalose and branched chain fatty acids, namely phthioceranic or hydroxy phthioceranic acid for SL and mycolic acid for TDM. A difference between SL and TDM is the occurrence of sulfate group in the trehalose moiety of SL, but not of TDM. So, SL is a characteristic anionic glycolipid, while TDM is a neutral glycolipid, respectively.

SL has long been reported to be correlated with virulence [4,5], and the virulence mechanism has been proposed to include inhibition of phagosome–lysosome fusion [6], suppression of priming for enhanced release of superoxide by lipopolysaccharide (LPS), IFN-γ, interleukin-1β and TNF-α [7,8], and self-damage of phagocytes by the release of superoxide [9]. On the other hand, since association of strains showing cord like growth with virulence has been recognized early in the history of mycobacterial research [10], TDM, the principle molecule for cord-formation, subsequently has shown the both edges of the sword such as granulomatogenicity [11–14], induction activity of chemotactic factors [15–18], anti-tumor activity [19–21], Th-1 type immuno adjuvant activity [16,17,20,22,23], inducibility of thymic atrophy [24,25] and lethal toxicity [15,26–28]. However to date, the virulence mechanism related to the both glycolipids has not been elucidated, although the structure resembles each other in possessing acyl trehalose moiety.

* Corresponding author. Tel.: +81 424 91 0611; fax: +81 424 92 9752.
E-mail address: y-fujita@bcg.gr.jp (Y. Fujita).

0882-4010/$ - see front matter © 2006 Elsevier Ltd. All rights reserved.
doi:10.1016/j.micpath.2006.02.002

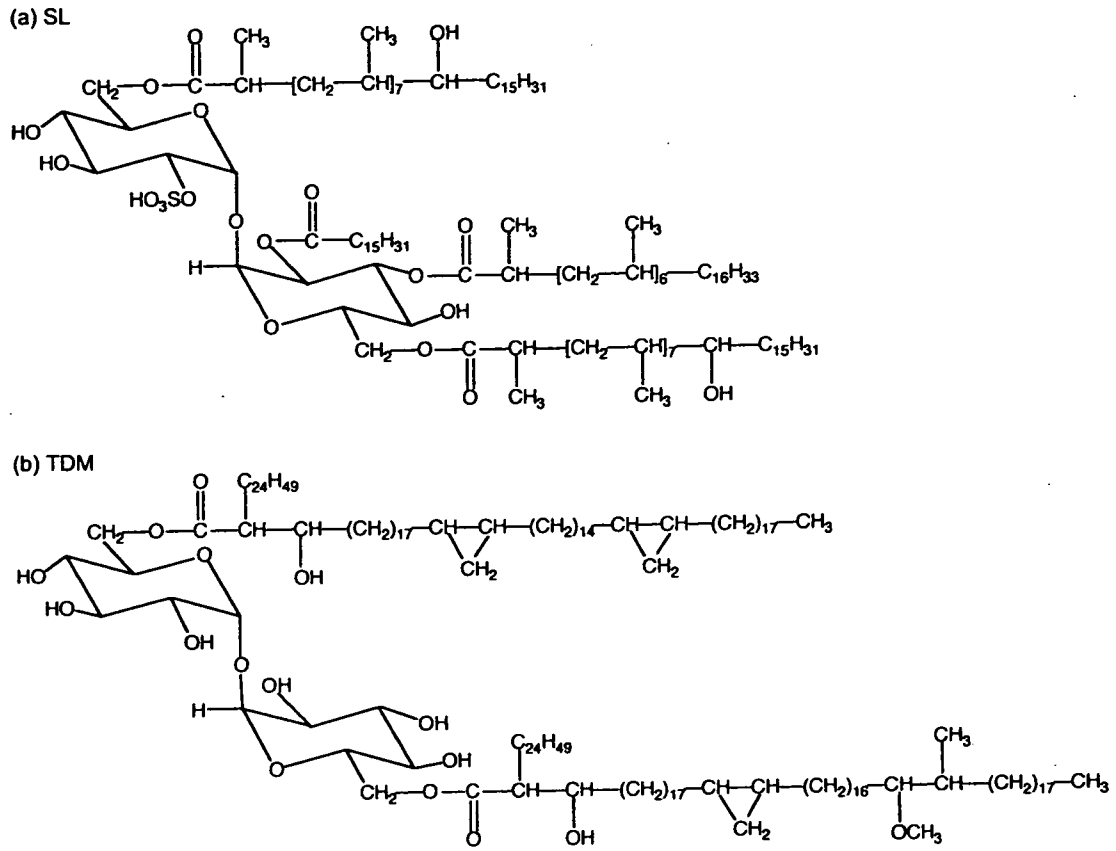

Fig. 1. Structure of SL and TDM from *M. tuberculosis* Aoyama B. (a) SL contained one molecule of palmitic, phthioceranic and two molecules of hydroxy phthioceranic acid ranging from C_{36} to C_{46}, and the total mass number ranged from *m/z* 2100 to 2750. (b) TDM contained two molecules of mycolic acids from any of alpha-, methoxy- or keto-mycolic acid with the carbon chains ranging from C_{76} to C_{92}, and the total mass number ranged from *m/z* 2600 to 3000.

Recently, there have been reported that highly transmissible *M. tuberculosis* strains inducible vigorous host responses are not necessarily highly virulent [29–31], and suggested that certain *M. tuberculosis* strain with high pathogenicity produce lipids that fail to efficiently induce the cytokine dependent Th-1 type protective immune response [32]. We have intended to reveal whether SL may affect directly or indirectly to the host immune response as a virulence factor of highly pathogenic strain of *M. tuberculosis*. Consequently, the presence of TDM alerts the immune system and therefore might be detrimental to mycobacterial survival in the host, while SL seems to be a specific virulence factor which suppresses the host protective activity of TDM.

2. Results

2.1. Toxicity and granuloma forming activity of TDM and SL

We first examined the time course changes in body weight for evaluating the toxicities of TDM and SL after i.v. injection in w/o/w-emulsions of each glycolipid or vehicle controls. Body weights were comparable on day 1 in all groups. By day 7 a clear increase was observed in control and SL injected groups (Fig. 3(a)). In contrast, the values of mice which had received injections of TDM were not increased as all animals suffered from peritonitis and concomitant diarrhoea. At the last

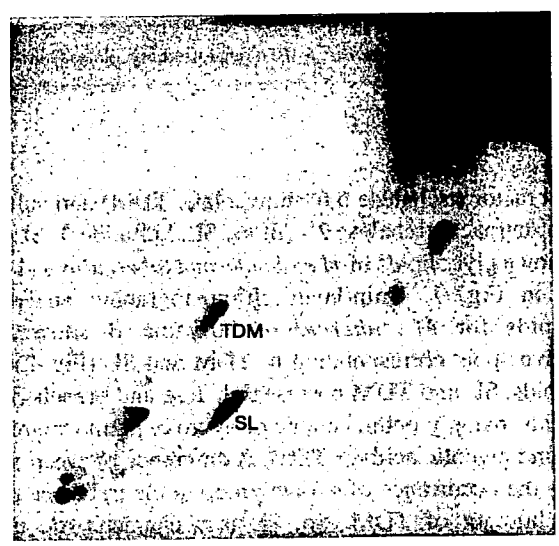

Fig. 2. Two-dimensional thin-layer chromatogram of glycolipids from *M. tuberculosis* Aoyama B. Total extractable lipids (100 μg) were developed with chloroform/methanol/water (90:10:1, by vol.; first dimension, upper) and chloroform/methanol/acetone/acetic acid (90:10:6:1, by vol.; second dimension, horizontal). Glycolipid spots were visualized with a 9 M H_2SO_4 spray followed by charring at 200 °C. Relative amount of SL to TDM was shown to be approximately same or little higher.

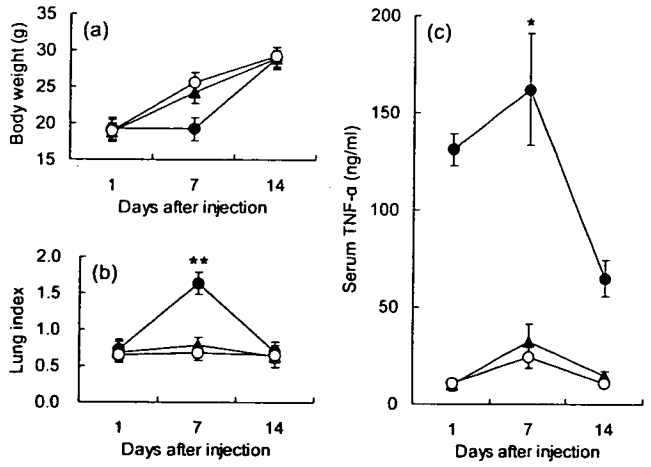

Fig. 3. Time course changes in body weight, lung index and serum TNF-α level after i.v. injection of TDM or SL. Mice received an i.v. injection of 300 μg TDM (closed circles ●), SL (triangles ▲) or the w/o/w-vehicle (open circles ○). Body and organ weights and serum TNF-α level were estimated on the indicated days. (a) Body weights; (b) lung indices; lung index of mouse injected with TDM on day 7 was significantly increased compared with that of SL injected mouse (**$P<0.01$); (c) serum TNF-α level; TNF-α level in mouse sera after priming with TDM and eliciting with LPS was significantly higher than that after priming with SL and eliciting with LPS (*$P<0.05$).

measurement at day 14, SL injected and control groups had additionally increased their body weights, while TDM injected group had overcome the toxic effects of this substance and also had a body weight comparable to that of the other groups. On day 7, TDM caused a marked increase in lung index compared to a slight increase in SL injected group (Fig. 3(b)). By day 14, the indices of both groups had returned to that of the control group. To correlate both the observed toxic effect of TDM and granuloma formation with a potential mediator, we measured TNF-α release in TDM- or SL-primed mice before triggering with LPS. Serum TNF-α concentration of SL-primed group were indistinguishable from those of control group, whereas a marked elevation was observed on day 7 after injection in TDM-primed group (Fig. 3(c)).

2.2. Histological findings on the antagonistic effect of SL upon the TDM-induced granuloma formation

As shown in above data, TDM and SL exhibited different biological activities in granulomatogenic responses, despite of the similar structure, we co-administered the both TDM and SL. Lung granuloma formation with i.v. injection of TDM was clearly dose responsive up to 300 μg/mouse. Histologically, i.v. injection of 300 μg TDM generated multiple massive granulomas widely in the both lung lobes with a marked infiltration of mature or immature macrophages and lymphocytes, and the heavily thickening of the alveolar interstitial tissues was observed (Fig. 4(c)). Co-administration of 300 μg TDM and 100 μg SL showed a slight inhibition of TDM-induced cellular infiltration, especially of macrophages and the resultant suppression of granuloma formation (Fig. 4(d)). Interestingly, co-administration of each 300 μg TDM and 300 μg SL showed a dramatical inhibition for granulomatous infiltration in lungs of mice near to the vehicle control level (Fig. 4(e)). However, single injection of SL did not show any massive granulomatous changes in lungs (Fig. 4(b)). Notably, for the highest inhibition with SL on TDM-induced granuloma formation simultaneous administration of the both glycolipids was essential (Fig. 4(e)), and SL injection at one hour before and after TDM injection lost the highly inhibitory effect of SL (Fig. 4(f)). These inhibitory effect of SL on TDM-induced granuloma formation in vivo was confirmed by lung and splenic index changes, as shown in Fig. 5(a) and (b). In both organs, increases in organ indices with 300 μg TDM injection were clearly inhibited by co-administration of 300 μg SL.

2.3. Paralleled inhibition of TDM-induced granuloma formation and TNF-α release by SL in vivo

Further interest is the inhibitory effect of SL on the TDM-induced granuloma formation and TNF-α release in mice. Addressing this issue in a more detailed experimental setting, we indeed confirmed that the presence of SL inhibited TDM-induced TNF-α release clearly in a dose-dependent manner (Fig. 6(a)). In parallel to the inhibition of TNF-α generation by SL, lung indices declined with increasing amounts of SL, and in mouse system co-administrated with 300 μg TDM and 300 μg SL the observed reduction was statistically significant (Fig. 6(b)). In additional experiments, we studied the time-dependency of the antagonistic effect of SL and found that simultaneous administration with the both glycolipids was necessary (Fig. 5). Injection of SL one hour before or after TDM injection was not sufficient to rescue mice from TDM-induced effects (subsequent loss or delayed gain of body weight, increase of lung index and high TNF-α levels).

2.4. TNF-α release by macrophages from ICR mice in response to TDM in vitro

To investigate the mechanism of the in vivo effects of SL on a cellular level, we first determined the release of TNF-α by alveolar macrophages (AM) and peritoneal macrophages (PM) with TDM stimulation. Harvesting culture supernatants after 24 h, we found highly elevated levels of TNF-α after incubation of AM in wells coated with various amounts of TDM in the range between 0 and 20 μg/well (Fig. 7(a)). In supernatants collected after 72 h also TNF-α concentrations in wells with 0.8 and 4.0 μg TDM showed clear increases from the background levels. Clear dose response curves were observed with TDM concentration between 0.032 and 0.8 μg in both cases of 24 and 72 h incubation of AM, although TNF-α concentration in the supernatant from PM was lower (Fig. 7(b)).

2.5. Antagonistic effect of SL on TDM-induced TNF-α release by macrophages from ICR mice in vitro

To model the in vivo TDM and SL co-administration experiments, the studies were carried out in the wells coated with both TDM and SL (Fig. 8(a)). AM were used because in

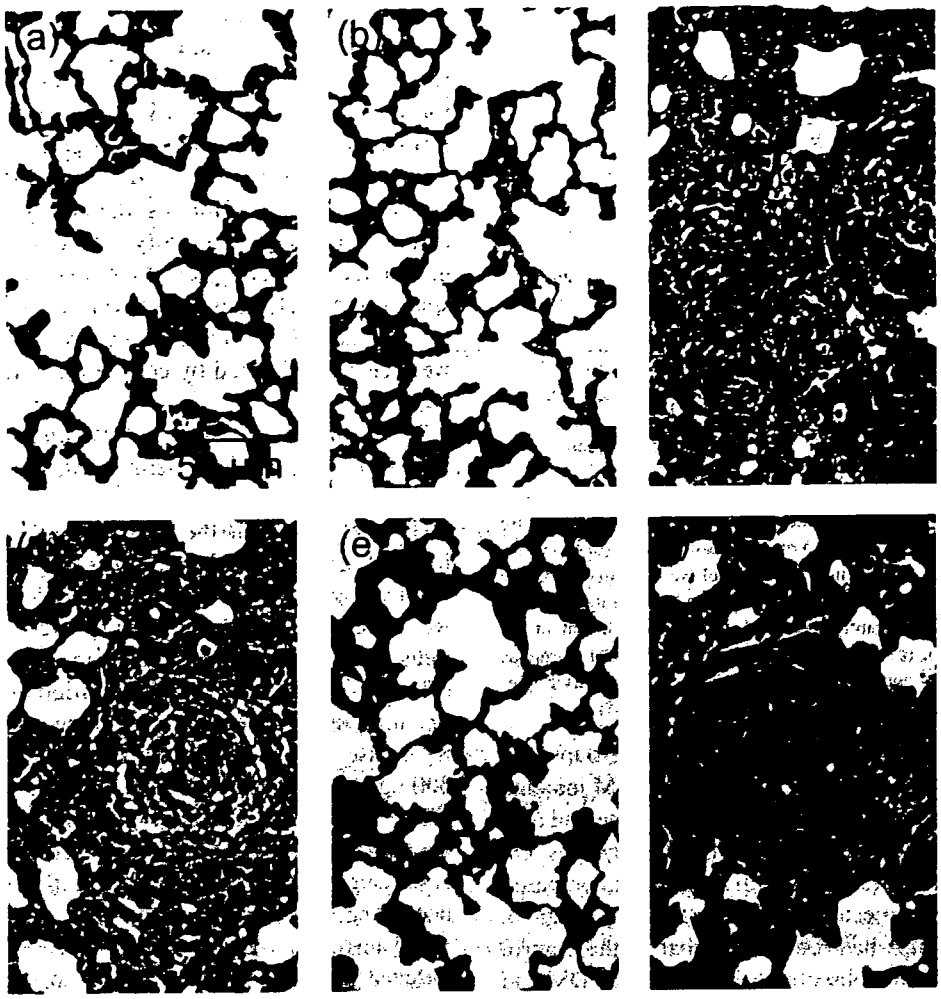

Fig. 4. Histological observation of lung granuloma formation by single or co-administration of TDM and/or SL in mice (H-E stain). (a) Control; (b) SL (300 μg/mouse); (c) TDM (300 μg/mouse); (d) TDM + SL (simultaneous co-administration of both TDM (300 μg/mouse) and SL (100 μg/mouse)); (e) TDM + SL (simultaneous co-administration of both TDM (300 μg/mouse) and SL (300 μg/mouse)); (f) TDM → SL (SL (300 μg/mouse) was injected 1 h after injection of TDM (300 μg/mouse)). Magnification, ×200.

contrast to PM they had been exposed and stimulated with the external foreign antigens and clearly TDM-responsive, thereby probably reflecting the importance of lung as entry site of *M. tuberculosis*, main target organ and consequently primary site of the defense. As maximum TDM-dependent TNF-α release had been observed in the wells coated with 0.8 μg TDM in the preceding experiment (Fig. 7(a)), this fixed value was tested together with increasing amounts of SL. In the range of 0.8–20 μg SL/well TNF-α production was reduced in a clearly dose-dependent way until maximum inhibition occurred at 4.0 μg (Fig. 8(a)).

2.6. Strain specificity of the antagonistic effect of SL

To determine if the observed effect of SL on TNF-α release depends on the genetic background of mice, the in vitro experiments were carried out with AM isolated from ICR, BALB/c and C3H/HeN mice, each of which differed in the sensitivity of granulomatogenicity to TDM, as reported previously [33]. Co-incubation with 0.8 μg TDM and 4.0 μg SL showed marked decreases in TNF-α release than incubation with 0.8 μg TDM solely in all cases (Fig. 8(b)). Since, all the mouse strains showed the similar tendencies in SL inhibition to TDM dependent TNF-α release in vitro, we concluded that the underlying mechanism is independent from the genetic factors which determine the susceptibility of the mouse strains to TDM-induced granuloma formation.

3. Discussion

Mycobacterial cell wall components have been shown to affect the immune response by modulating diverse cytokine patterns [34–36]. Among such components, TDM and SL, both being major components and having acyl trehalose moiety, have been focused from the aspect of virulence-associated factors. However, TDM has been recognized to be ubiquitous component distributed widely among pathogenic and non-pathogenic mycobacteria, while SL to be detected in only virulent strains isolated from human specimens [5,37–39]. Therefore, we have postulated that the structure and virulence activity relationship may be critically important. Studying on TDM-induced hypersensitivity to endotoxin shock, we

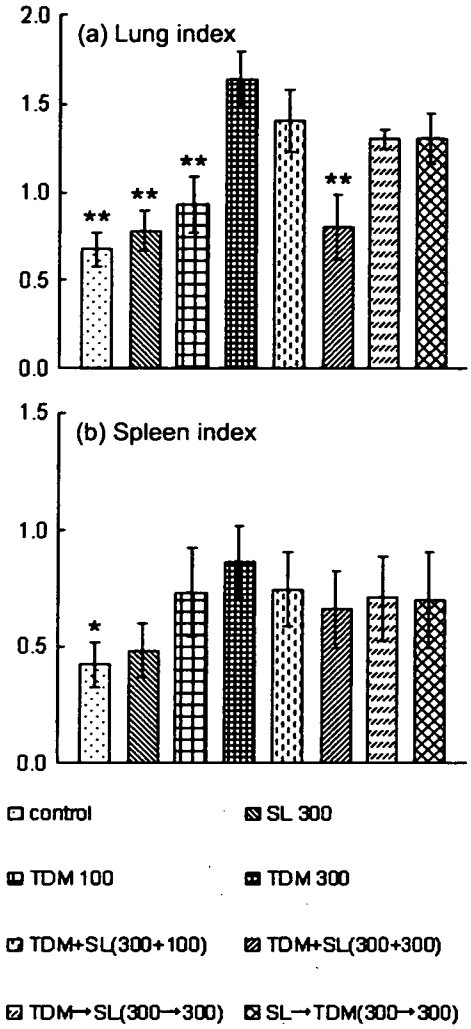

Fig. 5. Inhibition of TDM-induced granuloma formation by co-administration of SL assessed by lung or splenic indices in mice. Body and organ weights were estimated on day 7 after injection of glycolipids, and then lung and spleen indices were calculated. The asterisks *, indicate a P-value of <0.05 and **, indicate a P-value of <0.01 compared to 300 μg TDM injected mice.

previously obtained indications that SL might directly antagonize certain TDM effects [40]. In our present study, we therefore investigated the combined effect of TDM and SL on the granuloma formation and TNF-α release in mice. In vivo experiments demonstrated that the increase in TNF-α release and concomitantly higher granulomatous changes or lung indices after TDM injection. SL acted neutrally when delivered individually, but antagonistically by co-administration with TDM, and consequently decreased TNF-α levels and reduced lung indices towards normal values. Likewise, in vitro studies presented a coherent picture fitting to the in vivo results. AM responded well to TDM for TNF-α production, thus providing one explanation for the particular propensity of this organ for TDM-induced granuloma formation. SL, which by itself did not cause release of TNF-α, clearly blocked the induction of this cytokine with TDM in in vitro experiments.

The importance of TNF-α in host defense mechanism against mycobacterial infection has been vigorously investigated, and the reduction of granuloma formation and bactericidal mechanism and alteration of the mycobacterium-induced Th-1 type immune response have been reported in TNF-α blocked mice [41–46]. It is also known that blocking of TNF-α by anti-TNF-α antibodies resulted in rapid death of infected mice, delayed production of bactericidal nitric oxide and impaired containment of bacteria in granulomas [43]. By antagonizing TNF-α release, mycobacteria would therefore ensure a more hospitable environment. The potential clinical significance of our results becomes clear in the context of observations made by various groups in the past years: Flynn et al. demonstrated continuous expression of TNF-α during quiescent infection [47], and Adams et al. showed that neutralization of TNF-α by over expression of the extracellular domain of the TNF-α receptor exacerbated both acute and chronic infection [48]. Recently, a detailed study about the effects of TNF-α neutralization during latent tuberculosis revealed numerous histological changes including disorganization of granulomas, diffuse infiltration of inflammatory cells and increased apoptosis [49]. Considering the obvious importance of TNF-α for properly organized granulomas and

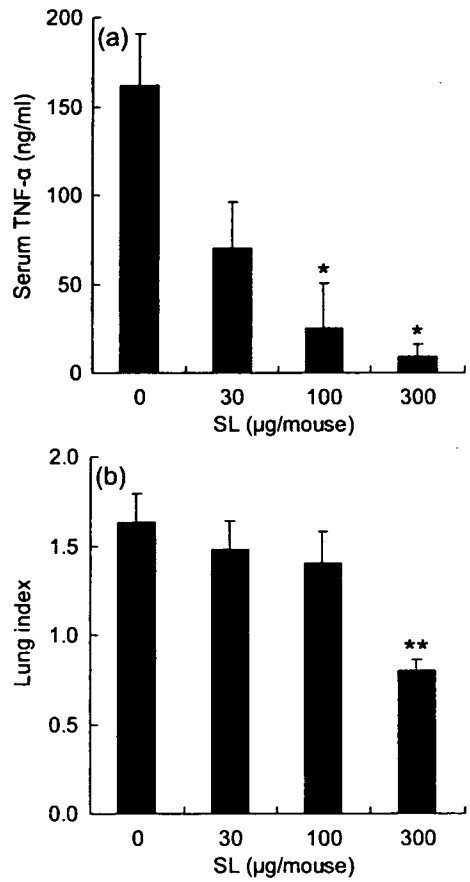

Fig. 6. Dose responsive inhibition of serum TNF-α induction and TDM-induced granuloma formation by SL. Mice were received co-administration of 300 μg TDM and 0, 30, 100 or 300 μg SL intravenously in w/o/w micelles. (a) Serum TNF-α release was triggered by i.v. injection of 100 μg LPS on day 7 post injection of TDM with or without of SL and sera were taken 2 h later. The asterisks *, indicate a P-value of <0.05 compared to 300 μg TDM injected mice. (b) On day 7 body and organ weights of all mice were measured for determination of lung indices. The asterisk **, indicate a P-value of <0.01 compared to 300 μg TDM injected mice.

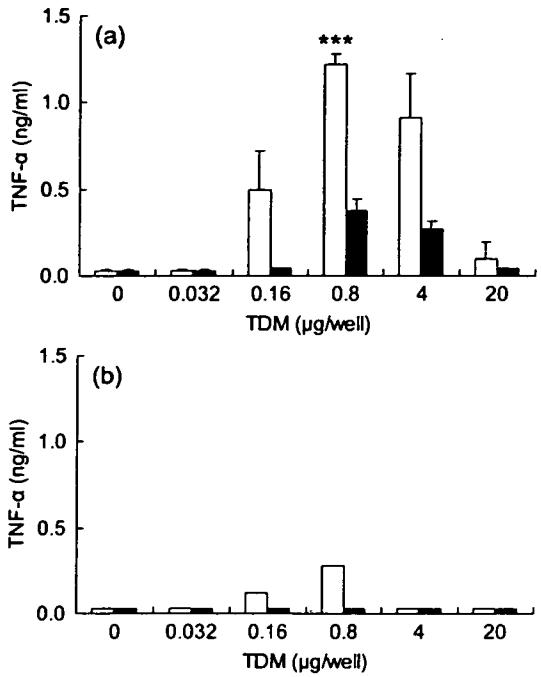

Fig. 7. In vitro effect of TDM on serum TNF-α production in alveolar or peritoneal macrophages in mice (a) and (b); wells were coated with the indicated amounts of TDM and the solvent was dried up completely. AM (a) or PM (b) (5.0×10^5 cells) were added in eaoh well. After 24 h (white bars) or 72 h (black bars) supernatants were collected and assayed for TNF-α. TDM-induced TNF-α production by AM was significantly higher than that from PM (***$P<0.001$).

thus for containment as prerequisite for effective suppression of mycobacteria, the potential significance of a TNF-α-blocking mechanism for *M. tuberculosis* is evident. In view of these data it is interesting that already decades ago Gangadharam et al. linked the virulence of Indian and British strains of *M. tuberculosis* to their SL content [4,5]. They showed highly virulent strain of *M. tuberculosis* human isolates contained higher amount of acidic glycolipids, and later the conclusion was confirmed by Goren et al. after application of more stringent methods for the isolation of SL [37].

SL was initially isolated from the virulent laboratory strain *M. tuberculosis* $H_{37}Rv$ but absent from the avirulent strain *M. tuberculosis* $H_{37}Ra$ [50]. Since then, the most highly virulent strain of *M. tuberculosis* have been reported generally to produce SL. In such virulent strains of *M. tuberculosis*, relative amount of SL to TDM is around comparable or higher than that of TDM (Fig. 2) and SL is more unstable than TDM [3], and in the administration study, most of investigators used 100–300 μg TDM in w/o/w micelles intravenously in mice for granuloma formation model [11–14]. We do not necessarily require such large amount of glycolipids for the experimental study, but we considered that these amounts of administration give the most reliable results. Initially, we have expected that SL may have a direct inhibitory effect against granulomatous response and TNF-α release, however, after co-administration, SL inhibited these responses indirectly via the TDM stimulation in vivo and in vitro. Thus, taken together, the suppression of TDM-induced TNF-α production and the inhibition of granuloma formation might constitute a new virulence function for SL.

Recently, Rousseau et al. showed that SL deficiency dose not significantly affect the replication, persistence and pathogenicity of *M. tuberculosis* $H_{37}Rv$ in mice and guinea pigs or in cultured macrophages, using a *pks* 2 knockout strain of *M. tuberculosis* $H_{37}Rv$ [51]. This mutant strain lacked the synthesis of phthioceranic and hydroxyl phthioceranic acids and consequently lacked SL, and further possibly devoided of the virulence attenuation factors [52]. One reason of the difference between two set of pairs; $H_{37}Rv$ and $H_{37}Ra$ or $H_{37}Rv$ (wild) and $H_{37}Rv$ *pks* 2 is that virulence is a complex phenotypic trait, and it may be possible that other factors in the *M. tuberculosis* $H_{37}Rv$ SL-deficient mutant compensate for the lack of SL. Therefore, further studies on the virulence analysis of recent clinical isolates will be necessary to clarify the role of SL.

The mechanism for inhibitory effect of SL on TDM-induced granuloma formation and TNF-α induction is not entirely known at the present stage. However, since the present study showed that the structure similarity of the both glycolipids existed distinctively, the simultaneous administration of TDM and SL to mice was necessary for the inhibitory effect, and the paralleled inhibition was observed by SL of TDM-induced TNF-α generation and granuloma formation in vivo and in vitro in dose dependent manner, there is a strong possibility

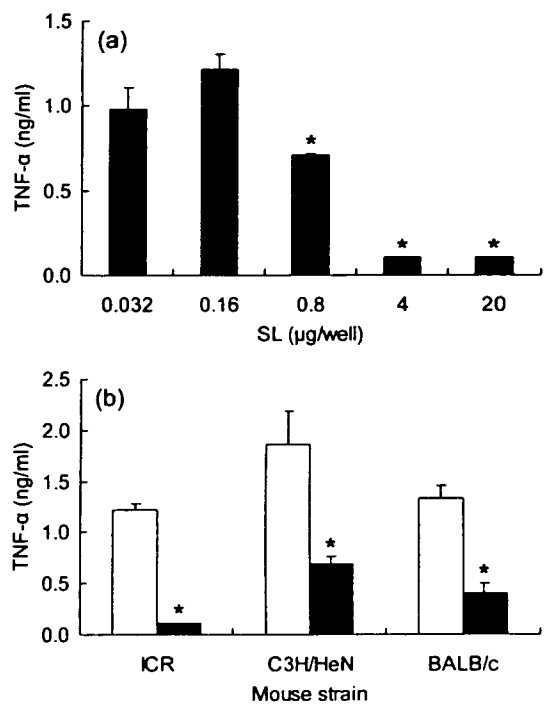

Fig. 8. In vitro effect of TDM and SL on serum TNF-α production in alveolar macrophages in mice. (a) AM were co-incubated in wells which contained 0.8 μg TDM and in addition the indicated amounts of SL. Supernatants were collected 24 h later and TNF-α concentrations were determined. The asterisk *, indicate a P-value of <0.05 compared to AM co-stimulated with 0.8 μg TDM and 0.032 μg SL. (b) AM were isolated from ICR, C3H/HeN and BALB/c mice and co-incubated in wells simultaneously coated with 0.8 μg TDM (white bars) or 0.8 μg TDM and 4.0 μg SL (black bars). Supernatants were collected after 24 h and assayed for TNF-α. In each strain of mice SL inhibited TDM-induced TNF-α production by AM (*$P<0.05$).

of a competitive inhibition of these two glycolipids against receptor binding site or macrophage activating step(s). In such context, identification of specific receptor(s) such as Toll-like receptor (TLR) or other signal transduction systems recently reported should be clarified in near future.

4. Materials and methods

4.1. Mice

Male BALB/c, C3H/HeN and ICR mice were purchased from Japan SLC Co., Shizuoka, Japan. All animals were 4-week-old at the start of the experiments and were kept under specific pathogen-free conditions.

4.2. Glycolipids

SL and TDM from *M. tuberculosis* Aoyama B were fractionated from the total extractable lipids, and were isolated and formulated as water/oil/water (w/o/w)-emulsions as described previously [40,53]. Total mass numbers of each SL and TDM were determined by matrix assisted laser desorption ionization-time of flight (MALDI-TOF) mass spectrometric analysis.

4.3. In vivo determination of TNF-α level after TDM and/or SL injection

For determination of serum TNF-α, ICR mice (five animals per group) were injected into the tail vein with 300 μg of TDM or SL as w/o/w-emulsions, and then stimulated on days 1, 7 or 14 by an intravenous injection of 100 μg *Salmonella minnesota* LPS (Difco Co.). Sera were collected 2 h later and TNF-α concentrations were determined in an assay using L929 cells as described elsewhere [54,55]. Quantitative results were derived from a calibration curve based on recombinant TNF-α (Genyzme).

For studying the effects of co-administration, ICR mice (five animals per group) were injected into the tail vein with 300 μg TDM together with 0, 30, 100 or 300 μg SL. After determination of body weights, stimulation with LPS on day 7 was performed as described above. Sera were taken 2 h later and lungs were removed for determination of lung indices.

4.4. Granuloma formation and determination of organ indices

ICR mice were injected into the tail vein with TDM and/or SL in w/o/w-emulsions or the vehicle control alone. On the indicated time points body weights and the weights of the isolated organs were determined. Organ indices were calculated according to the following formula: organ index is (organ weight/body weight) $\times 100$.

4.5. Histology

Samples from the lungs of mice 1 week after injection into the tail vein with TDM and/or SL in w/o/w-emulsions or the vehicle control alone were fixed with 10% formalin for 5 days, dehydrated, and embedded in paraffin. Sections were stained with hematoxylin and eosin.

4.6. Isolation of alveolar and peritoneal macrophages

For isolation of AM, 1 ml PBS was injected into the bronchus of each 5 ICR, C3H/HeN or BALB/c mice per group. After the thoracic cavities were opened, AM were collected by pumping and centrifugation at 1000 rpm for 10 min. The procedure was repeated 4–6 times and pooled washes were combined and centrifuged. Erythrocytes were lysed by incubation in Tris–NH_4Cl-buffer, and after the washed cells were resuspended in RPMI1640 supplemented with 10% FCS at a concentration of 5×10^6 cells/ml. A macrophage content of at least 90% was confirmed by methylene blue staining. For isolation of PM, 5 ICR mice per group received an intraperitoneal injection of 2.0 ml of 20% protease peptone. Four days later PM was harvested by flushing the peritoneal cavity twice with 5 ml PBS.

4.7. In vitro stimulation of alveolar and peritoneal macrophages for TNF-α production in TDM and/or SL coated wells

For studying the effect of stimulation of TDM in vitro, 50 μl hexane solution containing 0, 0.032, 0.16, 0.8, 4 or 20 μg TDM were added into wells of 96-well plates and kept in clean benches until the solvent was evaporated off. Similarly, for studying the effect of co-stimulation of TDM and SL, 50 μl hexane solution containing 0.8 μg TDM and 0.032, 0.16, 0.8, 4 or 20 μg SL were added into wells. 5×10^6AM or PM from ICR, C3H/HeN or BALB/c mice were added in a volume of 200 μl. After adhesion LPS was added at a final concentration of 1.6 μg/ml, cells were incubated at 37 °C for 24 or 72 h, and then culture supernatants were collected and stored at −80 °C until use.

4.8. Statistical analysis

Results are from $n=5$ mice and are from one representative experiment of three independent experiments of in vivo. Samples of in vitro cultures are from $n=5$ mice and are assayed in triplicate and represented a total of three independent experiments. The data represent the means ± SD. For statistical analysis the unpaired Student's *t*-test was used.

References

[1] Bloch H. Studies on the virulence of tubercle bacilli; isolation and biological properties of a constituent of virulent organisms. J Exp Med 1950;91:197–218.
[2] Noll H, Bloch H, Asselineau J, Lederer E. The chemical structure of the cord factor of *Mycobacterium tuberculosis*. Biochim Biophys Acta 1956; 20:299–309.
[3] Goren MB, Brokl O, Das BC. Sulfatides of *Mycobacterium tuberculosis*: the structure of the principal sulfatide (SL-I). Biochemistry 1976;15: 2728–35.

[4] Gangadharam PR, Cohn ML, Davis CL, Middlebrook G. Infectivity and pathogenicity of Indian and British strains of tubercle bacilli studied by aerogenic infection of guinea pigs. Am Rev Respir Dis 1963;87:200–5.
[5] Gangadharam PR, Cohn ML, Middlebrook G. Infectivity, pathogenicity and sulpholipid fraction of some Indian and British strains of tubercle bacilli. Tubercle 1963;44:452–5.
[6] Goren MB, D'Arcy Hart P, Young MR, Armstrong JA. Prevention of phagosome–lysosome fusion in cultured macrophages by sulfatides of *Mycobacterium tuberculosis*. Proc Natl Acad Sci USA 1976;73:2510–4.
[7] Brozna JP, Horan M, Rademacher JM, Pabst KM, Pabst MJ. Monocyte responses to sulfatide from *Mycobacterium tuberculosis*: inhibition of priming for enhanced release of superoxide, associated with increased secretion of interleukin-1 and tumor necrosis factor alpha, and altered protein phosphorylation. Infect Immun 1991;59:2542–8.
[8] Pabst MJ, Gross JM, Brozna JP, Goren MB. Inhibition of macrophage priming by sulfatide from *Mycobacterium tuberculosis*. J Immunol 1988; 140:634–40.
[9] Zhang L, Goren MB, Holzer TJ, Andersen BR. Effect of *Mycobacterium tuberculosis*-derived sulfolipid I on human phagocytic cells. Infect Immun 1988;56:2876–83.
[10] Middlebrook G, Dubos RJ, Pierce CJ. Virulence and morphological characteristics of mammalian tubercle bacilli. J Exp Med 1947;86: 175–87.
[11] Yarkoni E, Rapp HJ. Granuloma formation in lungs of mice after intravenous administration of emulsified trehalose-6,6′-dimycolate (cord factor): reaction intensity depends on size distribution of the oil droplets. Infect Immun 1977;18:552–4.
[12] Kunkel SL, Chensue SW, Strieter RM, Lynch JP, Remick DG. Cellular and molecular aspects of granulomatous inflammation. Am J Respir Cell Mol Biol 1989;1:439–47.
[13] Orme IM. The immunopathogenesis of tuberculosis: a new working hypothesis. Trends Microbiol 1998;6:94–7.
[14] Kaneda K, Sumi Y, Kurano F, Kato Y, Yano I. Granuloma formation and hemopoiesis induced by C_{36-48}-mycolic acid-containing glycolipids from *Nocardia rubra*. Infect Immun 1986;54:869–75.
[15] Matsunaga I, Oka S, Fujiwara N, Yano I. Relationship between induction of macrophage chemotactic factors and formation of granulomas caused by mycoloyl glycolipids from *Rhodococcus ruber* (*Nocardia rubra*). J Biochem Tokyo 1996;120:663–70.
[16] Yamagami H, Matsumoto T, Fujiwara N, Arakawa T, Kaneda K, Yano I, et al. Trehalose 6,6′-dimycolate (cord factor) of *Mycobacterium tuberculosis* induces foreign-body- and hypersensitivity-type granulomas in mice. Infect Immun 2001;69:810–5.
[17] Lima VM, Bonato VL, Lima KM, Dos Santos SA, Dos Santos RR, Goncalves ED, et al. Role of trehalose dimycolate in recruitment of cells and modulation of production of cytokines and NO in tuberculosis. Infect Immun 2001;69:5305–12.
[18] Behling CA, Perez RL, Kidd MR, Staton Jr GW, Hunter RL. Induction of pulmonary granulomas, macrophage procoagulant activity, and tumor necrosis factor-alpha by trehalose glycolipids. Ann Clin Lab Sci 1993;23: 256–66.
[19] Bekierkunst A, Levij IS, Yarkoni E. Suppression of urethan-induced lung adenomas in mice treated with trehalose-6,6-dimycolate (cord factor) and living bacillus Calmette Guerin. Science 1971;174:1240–2.
[20] Furukawa M, Ohtsubo Y, Sugimoto N, Katoh Y, Dohi Y. Induction of tumoricidal activated macrophages by a liposome-encapsulated glycolipid, trehalose 2,3,6′-trimycolate from *Gordona aurantiaca*. FEMS Microbiol Immunol 1990;2:83–8.
[21] Orbach-Arbouys S, Tenu JP, Petit JF. Enhancement of in vitro and in vivo antitumor activity by cord factor (6-6′-dimycolate of trehalose) administered suspended in saline. Int Arch Allergy Appl Immunol 1983;71:67–73.
[22] Oswald IP, Dozois CM, Petit JF, Lemaire G. Interleukin-12 synthesis is a required step in trehalose dimycolate-induced activation of mouse peritoneal macrophages. Infect Immun 1997;65:1364–9.
[23] Ryll R, Watanabe K, Fujiwara N, Takimoto H, Hasunuma R, Kumazawa Y, et al. Mycobacterial cord factor, but not sulfolipid, causes depletion of NKT cells and upregulation of CD1d1 on murine macrophages. Microbes Infect 2001;3:611–9.
[24] Ozeki Y, Kaneda K, Fujiwara N, Morimoto M, Oka S, Yano I. In vivo induction of apoptosis in the thymus by administration of mycobacterial cord factor (trehalose 6,6′-dimycolate). Infect Immun 1997;65:1793–9.
[25] Hamasaki N, Isowa K, Kamada K, Terano Y, Matsumoto T, Arakawa T, et al. In vivo administration of mycobacterial cord factor (trehalose 6, 6′-dimycolate) can induce lung and liver granulomas and thymic atrophy in rabbits. Infect Immun 2000;68:3704–9.
[26] Ueda S, Fujiwara N, Naka T, Sakaguchi I, Ozeki Y, Yano I, et al. Structure-activity relationship of mycoloyl glycolipids derived from *Rhodococcus* sp. 4306. Microb Pathog 2001;30:91–9.
[27] Gotoh K, Mitsuyama M, Imaizumi S, Kawamura I, Yano I. Mycolic acid-containing glycolipid as a possible virulence factor of *Rhodococcus equi* for mice. Microbiol Immunol 1991;35:175–85.
[28] Dubnau E, Chan J, Raynaud C, Mohan VP, Laneelle MA, Yu K, et al. Oxygenated mycolic acids are necessary for virulence of *Mycobacterium tuberculosis* in mice. Mol Microbiol 2000;36:630–7.
[29] Valway SE, Sanchez MP, Shinnick TF, Orme I, Agerton T, Hoy D, et al. An outbreak involving extensive transmission of a virulent strain of *Mycobacterium tuberculosis*. N Engl J Med 1998;338:633–9.
[30] Manca C, Tsenova L, Barry III CE, Bergtold A, Freeman S, Haslett PA, et al. *Mycobacterium tuberculosis* CDC1551 induces a more vigorous host response in vivo and in vitro, but is not more virulent than other clinical isolates. J Immunol 1999;162:6740–6.
[31] Manca C, Tsenova L, Bergtold A, Freeman S, Tovey M, Musser JM, et al. Virulence of a *Mycobacterium tuberculosis* clinical isolate in mice is determined by failure to induce Th1 type immunity and is associated with induction of IFN-alpha/beta. Proc Natl Acad Sci USA 2001;98:5752–7.
[32] Manca C, Reed MB, Freeman S, Mathema B, Kreiswirth B, Barry III CE, et al. Differential monocyte activation underlies strain-specific *Mycobacterium tuberculosis* pathogenesis. Infect Immun 2004;72:5511–4.
[33] Sumi Y, Kurano S, Kato Y, Sawai H, Tomiyasu I, Kaneda K, et al. Strain differences in granuloma formation in mice in response to mycolic acid-containing glycolipids of some species of *Nocardia* and *Rhodococcus*. Nippon Saikingaku Zasshi 1986;41:797–804.
[34] Adams JL, Czuprynski CJ. Mycobacterial cell wall components induce the production of TNF-alpha, IL-1, and IL-6 by bovine monocytes and the murine macrophage cell line RAW 264.7. Microb Pathog 1994;16: 401–11.
[35] Adams JL, Czuprynski CJ. Ex vivo induction of TNF-alpha and IL-6 mRNA in bovine whole blood by *Mycobacterium paratuberculosis* and mycobacterial cell wall components. Microb Pathog 1995;19:19–29.
[36] Horgen L, Barrow EL, Barrow WW, Rastogi N. Exposure of human peripheral blood mononuclear cells to total lipids and serovar-specific glycopeptidolipids from *Mycobacterium avium* serovars 4 and 8 results in inhibition of TH1-type responses. Microb Pathog 2000;29:9–16.
[37] Goren MB, Brokl O, Schaefer WB. Lipids of putative relevance to virulence in *Mycobacterium tuberculosis*: correlation of virulence with elaboration of sulfatides and strongly acidic lipids. Infect Immun 1974;9: 142–9.
[38] Goren MB, Grange JM, Aber VR, Allen BW, Mitchison DA. Role of lipid content and hydrogen peroxide susceptibility in determining the guinea-pig virulence of *Mycobacterium tuberculosis*. Br J Exp Pathol 1982;63: 693–700.
[39] Grange JM, Aber VR, Allen BW, Mitchison DA, Goren MB. The correlation of bacteriophage types of *Mycobacterium tuberculosis* with guinea-pig virulence and in vitro-indicators of virulence. J Gen Microbiol 1978;108:1–7.
[40] Watanabe K, Hasunuma R, Horikoshi T, Yamana H, Maruyama H, Fujiwara N, et al. Induction of hypersensitivity to endotoxin lethality in mice by treatment with trehalose 6,6′-dimycolate but not with 2,3,6,6′-tetraacyl trehalose 2′-sulfate. J Endotoxin Res 1999;5:23–30.
[41] Bean AG, Roach DR, Briscoe H, France MP, Korner H, Sedgwick JD, et al. Structural deficiencies in granuloma formation in TNF gene-targeted mice underlie the heightened susceptibility to aerosol *Mycobacterium tuberculosis* infection, which is not compensated for by lymphotoxin. J Immunol 1999;162:3504–11.

[42] Ehlers S. Role of tumour necrosis factor (TNF) in host defence against tuberculosis: implications for immunotherapies targeting TNF. Ann Rheum Dis 2003;62:ii37–42.
[43] Flynn JL, Goldstein MM, Chan J, Triebold KJ, Pfeffer K, Lowenstein CJ, et al. Tumor necrosis factor-alpha is required in the protective immune response against *Mycobacterium tuberculosis* in mice. Immunity 1995;2: 561–72.
[44] Kaneko H, Yamada H, Mizuno S, Udagawa T, Kazumi Y, Sekikawa K, et al. Role of tumor necrosis factor-alpha in *Mycobacterium*-induced granuloma formation in tumor necrosis factor-alpha-deficient mice. Lab Invest 1999;79:379–86.
[45] Kindler V, Sappino AP, Grau GE, Piguet PF, Vassalli P. The inducing role of tumor necrosis factor in the development of bactericidal granulomas during BCG infection. Cell 1989;56:731–40.
[46] Roach DR, Bean AG, Demangel C, France MP, Briscoe H, Britton WJ. TNF regulates chemokine induction essential for cell recruitment, granuloma formation, and clearance of mycobacterial infection. J Immunol 2002;168:4620–7.
[47] Flynn JL, Scanga CA, Tanaka KE, Chan J. Effects of aminoguanidine on latent murine tuberculosis. J Immunol 1998;160:1796–803.
[48] Adams LB, Mason CM, Kolls JK, Scollard D, Krahenbuhl JL, Nelson S. Exacerbation of acute and chronic murine tuberculosis by administration of a tumor necrosis factor receptor-expressing adenovirus. J Infect Dis 1995;171:400–5.
[49] Mohan VP, Scanga CA, Yu K, Scott HM, Tanaka KE, Tsang E, et al. Effects of tumor necrosis factor alpha on host immune response in chronic persistent tuberculosis: possible role for limiting pathology. Infect Immun 2001;69:1847–55.
[50] Middlebrook G, Coleman CM, Schaefer WB. Sulfolipid from virulent tubercle bacilli. Proc Natl Acad Sci USA 1959;45:1801–4.
[51] Rousseau C, Turner OC, Rush E, Bordat Y, Sirakova TD, Kolattukudy PE, et al. Sulfolipid deficiency does not affect the virulence of *Mycobacterium tuberculosis* H37Rv in mice and guinea pigs. Infect Immun 2003;71:4684–90.
[52] Sirakova TD, Thirumala AK, Dubey VS, Sprecher H, Kolattukudy PE. The *Mycobacterium tuberculosis pks2* gene encodes the synthase for the hepta- and octamethyl-branched fatty acids required for sulfolipid synthesis. J Biol Chem 2001;276:16833–9.
[53] Yano I, Tomiyasu I, Kitabatake S, Kaneda K. Granuloma forming activity of mycolic acid-containing glycolipids in *Nocardia* and related taxa. Acta Leprol 1984;2:341–9.
[54] Carswell EA, Old LJ, Kassel RL, Green S, Fiore N, Williamson B. An endotoxin-induced serum factor that causes necrosis of tumors. Proc Natl Acad Sci USA 1975;72:3666–70.
[55] Aggarwal BB, Kohr WJ, Hass PE, Moffat B, Spencer SA, Henzel WJ, et al. Human tumor necrosis factor. Production, purification, and characterization. J Biol Chem 1985;260:2345–54.

Molecular Microbiology (2007) 63(4), 1096–1106

doi:10.1111/j.1365-2958.2006.05585.x
First published online 18 January 2007

Loss of a conserved 7-methylguanosine modification in 16S rRNA confers low-level streptomycin resistance in bacteria

Susumu Okamoto,[1] Aki Tamaru,[2] Chie Nakajima,[3] Kenji Nishimura,[1,4] Yukinori Tanaka,[1,4] Shinji Tokuyama,[4] Yasuhiko Suzuki[3] and Kozo Ochi[1]*

[1]*Microbial Function Laboratory, National Food Research Institute, 2-1-12 Kannondai, Tsukuba, Ibaraki 305-8642, Japan.*

[2]*Bacteriology Division, Osaka Prefectural Institute of Public Health, 1-3-69 Nakamichi, Higashinari-ku, Osaka 537-0025, Japan.*

[3]*Department of Global Epidemiology, Research Center for Zoonosis Control, Hokkaido University, Kita 18, Nishi 9, Kita-ku, Sapporo 060-0818, Japan.*

[4]*Department of Applied Biological Chemistry, Faculty of Agriculture, Shizuoka University, 836 Ohya, Shizuoka 422-8529, Japan.*

Summary

Streptomycin has been an important drug for the treatment of tuberculosis since its discovery in 1944. But numerous strains of *Mycobacterium tuberculosis*, the bacterial pathogen that causes tuberculosis, are now streptomycin resistant. Although such resistance is often mediated by mutations within *rrs*, a 16S rRNA gene or *rpsL*, which encodes the ribosomal protein S12, these mutations are found in a limited proportion of clinically isolated streptomycin-resistant *M. tuberculosis* strains. Here we have succeeded in identifying a mutation that confers low-level streptomycin resistance to bacteria, including *M. tuberculosis*. We found that mutations within the gene *gidB* confer low-level streptomycin resistance and are an important cause of resistance found in 33% of resistant *M. tuberculosis* isolates. We further clarified that the *gidB* gene encodes a conserved 7-methylguanosine (m^7G) methyltransferase specific for the 16S rRNA, apparently at position G527 located in the so-called 530 loop. Thus, we have identified *gidB* as a new streptomycin-resistance locus and uncovered a resistance mechanism that is mediated by loss of a conserved m^7G modification in 16S rRNA. The clinical significance of *M. tuberculosis gidB* mutation also is noteworthy, as *gidB* mutations emerge spontaneously at a high frequency of 10^{-6} and, once emerged, result in vigorous emergence of high-level streptomycin-resistant mutants at a frequency more than 2000 times greater than that seen in wild-type strains. Further studies on the precise function of GidB may provide a basis for developing strategies to suppress pathogenic bacteria, including *M. tuberculosis*.

Accepted 21 December, 2006. *For correspondence. E-mail kochi@affrc.go.jp; Tel. (+81) 29 838 8125; Fax (+81) 29 838 7996.

Introduction

Selman Waksman discovered streptomycin to be a particularly potent drug against *Mycobacterium tuberculosis* in 1944, while at Rutgers University (Schatz and Waksman, 1944). The first mutants resistant to streptomycin were reported as early as 1946 (Klein and Kimmelman, 1946). The mutants could be classified into two distinct types, depending upon whether they exhibit high- or low-level streptomycin resistance.

Because of its clinical importance, molecular mechanisms of resistance to streptomycin have been extensively studied, especially in *M. tuberculosis* (Finken *et al.*, 1993; Nair *et al.*, 1993; Honoré and Cole, 1994; Honoré *et al.*, 1995; Carter *et al.*, 2000; Ogle and Ramakrishnan, 2005). However, the genetic basis of resistance is still not fully understood. High-level streptomycin resistance is often linked to mutations within *rrs*, a 16S rRNA gene, or *rpsL*, which encodes the ribosomal protein S12 (Finken *et al.*, 1993; Nair *et al.*, 1993; Honoré and Cole, 1994; Honoré *et al.*, 1995). Most mutations within S12 that confer resistance to, or dependence on, streptomycin are known to lead to a hyperaccurate phenotype (Carter *et al.*, 2000), which compensates for the effect of the drug, without affecting the interaction between the drug and the ribosome. A number of mutations within 16S rRNA, including those within the so-called 530 loop, also lead to both streptomycin resistance and hyperaccuracy (Montandon *et al.*, 1986; Powers and Noller, 1991; Pinard *et al.*, 1993). Such changes, however, have been identified in a limited

Table 1. Frequency of *gidB* mutants in several bacteria.[a]

Strain	Sm concentration (μg ml^{-1})		Frequency of Sm^r mutants	Frequency of *gidB* mutants
	MIC	Mutant selection		
Escherichia coli	2	5	2.0×10^{-5}	4/39
Staphylococcus aureus	3	10	1.2×10^{-5}	4/16
Mycobacterium smegmatis	0.3	1	2.3×10^{-4}	17/18
Mycobacterium tuberculosis	1	2	2.8×10^{-6}	10/10

a. For mutant isolation, the media used were LB (for *E. coli* and *S. aureus*), R (for *M. smegmatis*) and Middlebrook 7H11 [for *M. tuberculosis* (No. 05–048)].
Sm, streptomycin; Sm^r, streptomycin resistant. Frequencies of *gidB* mutants are expressed as the (number of *gidB* mutants)/(number of Sm^r mutants sequenced).

proportion (i.e. just over one-half) of clinically isolated streptomycin-resistant *M. tuberculosis* strains studied to date (Meier *et al.*, 1996; Sreevatsan *et al.*, 1996; Gillespie, 2002; Ramaswamy *et al.*, 2004). Consequently, the mechanism underlying low-level resistance to streptomycin has remained obscure for 60 years (Demerec, 1948).

We describe here our identification of an unknown mutation within *gidB* that confers low-level streptomycin resistance. Subsequent analysis of this mutation demonstrated both its clinical importance and its potential to further our understanding of the mechanism underlying the development of high-level streptomycin resistance in *M. tuberculosis*, thus providing basis for developing strategies to suppress this serious pathogenic bacterium.

Results

Low-level streptomycin resistance caused by gidB *mutations*

Our laboratory has focused on unravelling unknown ribosomal functions, thus aiming to develop 'ribosome engineering' (Ochi *et al.*, 2004) as a rational approach to taking full advantage of bacterial capabilities. The members of the genus *Streptomyces* are distinguished in the ability to exert a wide variety of secondary metabolisms as represented by antibiotic production. The ability of *Streptomyces coelicolor* A3(2) to produce antibiotics is dramatically enhanced by introducing mutations that confer high- or low-level resistance to streptomycin (Shima *et al.*, 1996; Hosoya *et al.*, 1998; Okamoto *et al.*, 2003; Ochi *et al.*, 2004; Hosaka *et al.*, 2006). To study the mechanism by which mutations causing low-level streptomycin resistance induce gene activation, we first conducted genetic analysis (i.e. mapping of the mutations on the chromosome) (Ochi and Hosoya, 1998). Because of the apparent failure of conventional cloning strategies to identify the mutations, we next used comparative genome sequencing (CGS) (Albert *et al.*, 2005), a microarray hybridization-based method developed to search for single nucleotide polymorphisms (SNPs) and insertion–deletion sites within the genome. The mutant (*relA str-1*) strain, showing low-level streptomycin resistance due to *str-1* mutation, served for analysis. Because the *str-1* mutation had previously been mapped to the 7 o'clock position on the *S. coelicolor* chromosome (Ochi and Hosoya, 1998), CGS was conducted for 1.2 Mbp around the 7 o'clock region. This analysis enabled us to identify a putative SNP within the gene *gidB*, which was confirmed to be a deletion mutation (deletion of 488 A) by DNA sequencing (details will be reported elsewhere).

The *gidAB* operon was originally described in *Escherichia coli* in relation to glucose-mediated inhibition of cell division (von Meyenburg and Hansen, 1980). Subsequent analysis revealed that inactivation of *gidA* (but not *gidB*) is responsible for impaired cell division in the presence of glucose (von Meyenburg and Hansen, 1980), and more recent data support the involvement of *gidA* in tRNA modification (Brégeon *et al.*, 2001; Yim *et al.*, 2006). On the other hand, function of *gidB* has remained obscure to date. The *gidB* gene is highly conserved in both Gram-positive and Gram-negative bacteria (Fig. S1) and is found in all bacterial genomes sequenced to date, including that of *Mycoplasma genitalium*, the smallest genome of a known self-sustaining living organism. We therefore suspected that *gidB* mutations may cause low-level streptomycin resistance in virtually all bacteria. To address this possibility, we examined the emergence of streptomycin-resistant mutants in several bacteria on plates containing a low concentration of streptomycin [two to three times the minimum inhibitory concentration (MIC)] (Table 1). We found that streptomycin-resistant mutants emerged at a high frequency, in the order of 10^{-4} or 10^{-5}, in *E. coli*, *Staphylococcus aureus* and *Mycobacterium smegmatis*, and in the order of 10^{-6} in *M. tuberculosis* (Table 1). In addition, there was a high incidence of *gidB* mutations in these strains. For example, in *M. smegmatis* and *M. tuberculosis*, almost all mutants carried *gidB* mutations (17/18 and 10/10 respectively), including a variety of point, deletion and insertion mutations (see Table S1), suggesting loss of function of *gidB* may result in a streptomycin-resistant phenotype.

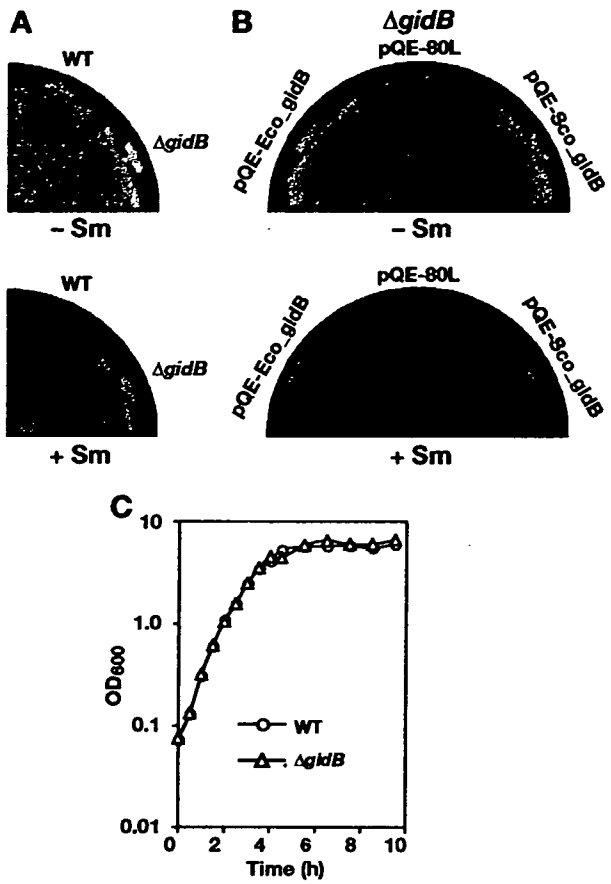

Fig. 1. Mutation of *gidB* confers streptomycin resistance.
A. Streptomycin-resistant phenotype of the *E. coli* Δ*gidB* mutant. Wild-type and Δ*gidB* strains were streaked onto LB (–Sm) or LB containing 10 μg ml^{-1} streptomycin (+Sm).
B. Complementation of the Δ*gidB* mutant. *E. coli* or *S. coelicolor* GidB was expressed as a His-tagged protein using pQE-80L. Strains were grown on LB agar containing ampicillin, either in the absence (–Sm) or presence (+Sm) of streptomycin (8 μg ml^{-1}).
C. Growth of Δ*gidB* mutant, as compared with the wild-type strain. Cultures were grown in LB medium at 37°C.

To verify a causal relationship between *gidB* mutation and streptomycin resistance, we compared wild-type *E. coli* BW25113 and its isogenic *gidB* deletion (Δ*gidB*) mutant. We found that the streptomycin MIC for the wild-type strain was 2 μg ml^{-1}, whereas the Δ*gidB* mutant remained viable at concentrations up to 15 μg ml^{-1}, suggesting that the *gidB* mutation is indeed responsible for streptomycin resistance (Fig. 1A). This was confirmed by our finding that introduction of a plasmid containing the wild-type *gidB* into Δ*gidB* cells completely eliminated the resistance to streptomycin (Fig. 1B). Likewise, *gidB* from *S. coelicolor* also effectively complemented the *E. coli* *gidB* mutation. Apparently, the proteins encoded by both *gidB* genes were functionally equivalent and involved in the same biochemical pathway(s). The *gidB* mutant also showed no changes in susceptibility to ribosome-targeting antibiotics, such as erythromycin, tetracycline, chloramphenicol and spectinomycin (data not shown).

Certain drug-resistant bacteria grow more slowly than susceptible bacteria because the mutations that confer resistance also reduce the overall fitness of the organism (Andersson and Levin, 1999), a phenomenon known as 'cost of resistance'. We found, however, that the *E. coli* Δ*gidB* mutant grew as well as the parent strain in both nutritional media (Fig. 1C) and chemically defined media (data not shown).

GidB functions as an rRNA methyltransferase

The GidB protein has a putative *S*-adenosyl-L-methionine (SAM)-binding motif within its primary structure (Fig. S1) (Kagan and Clarke, 1994), and the crystal structure of *E. coli* GidB showed that it contains a SAM-dependent methyltransferase fold within its ternary structure (Romanowski *et al.*, 2002). As streptomycin resistance often results from mutations that affect ribosome-associated components (Cundliffe, 1990), we hypothesized that *gidB* mutants also have an altered ribosome – i.e. a deficiency in the methylation of some ribosomal component(s), which generates streptomycin resistance. We tested this hypothesis by measuring the protein synthetic activity of ribosomes *in vitro* (Fig. 2). Green fluorescent protein (GFP) was synthesized using ribosomes and the S-150 fractions from the wild-type and the Δ*gidB*

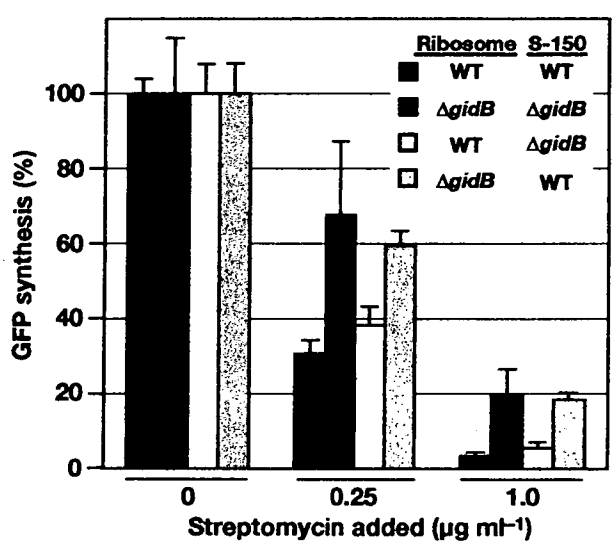

Fig. 2. Effect of streptomycin on *in vitro* protein synthesis. Ribosome and S-150 fractions were prepared from wild-type (streptomycin susceptible) and Δ*gidB* (streptomycin resistant) *E. coli* strains. Reactions were performed using the four possible combinations of ribosome and S-150 fractions. Streptomycin was added to the reaction mixture at the indicated concentrations. The production of GFP was measured, and the results are presented as the mean per cent translational activity ± SD, with 100% defined as activity in the absence of the drug.

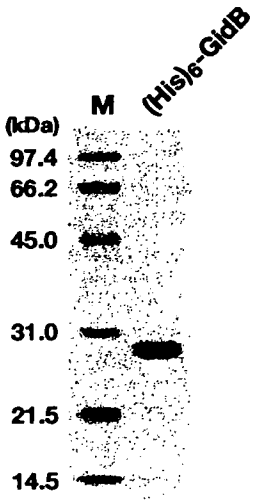

Fig. 3. SDS-PAGE of the purified $(His)_6$-GidB protein. Two micrograms of the protein was subjected to 12% SDS-PAGE. M represents marker proteins.

strains in the presence or absence of streptomycin. By cross-mixing the components, we determined that the ribosome itself, not the S-150 fraction, is responsible for streptomycin resistance.

We next determined the ribosomal target for the presumptive methyltransferase GidB. We therefore prepared an N-terminal His-tagged GidB and purified it using immobilized metal ion chromatography (Fig. 3). To determine whether the recombinant GidB was able to catalyse ribosomal modification, 70S ribosomes from the wild-type or Δ*gidB* strain were incubated in the presence of purified GidB and [*methyl*-^{3}H]SAM, and incorporation of methyl groups was analysed by trichloroacetic acid precipitation or fluorography of polyacrylamide gels. When ribosomes from Δ*gidB* cells were used as a substrate, a significant amount of methyl groups were incorporated (Fig. 4A). By contrast, no incorporation was detected when ribosomes from the wild-type cells were used, presumably reflecting the already saturated methylation status of those ribosomes. Moreover, using rRNA extraction and subsequent non-denaturing polyacrylamide gel electrophoresis, we determined that the methylated ribosomal component was the 16S rRNA (Fig. 4B). This was confirmed by per-

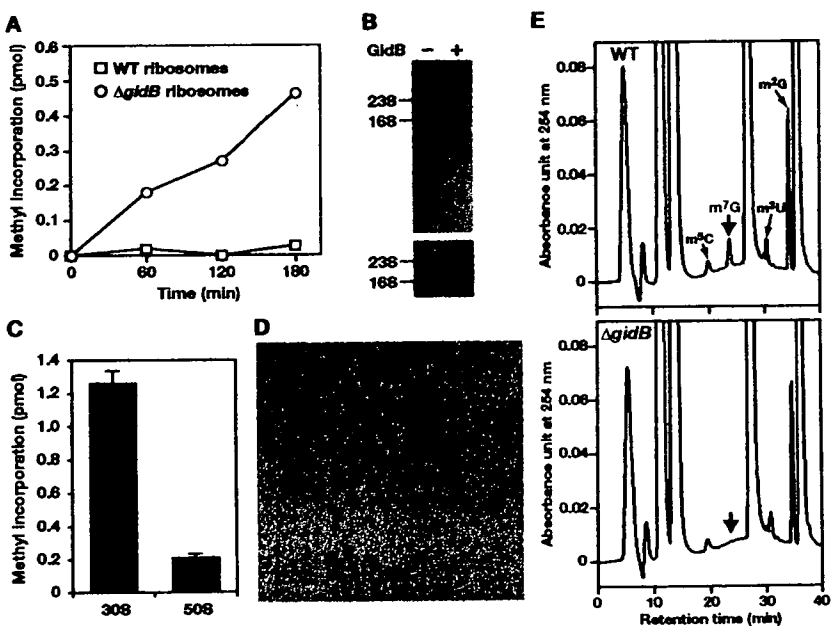

Fig. 4. GidB is a m^7G methyltransferase specific for 16S rRNA.
A. Methyl acceptor activity of wild-type and mutant ribosomes. 70S ribosomes (1 μM) prepared from either the wild-type (open squares) or Δ*gidB* (open circles) *E. coli* strain were subjected to methylation using [^{3}H]-SAM (3 μM) and the purified $(His)_6$-GidB protein (500 nM).
B. Methylation of 16S rRNA by GidB. Δ*gidB* 70S ribosomes were methylated using [^{3}H]-SAM and $(His)_6$-GidB, after which rRNAs were extracted and analysed on 3.5% non-denaturing polyacrylamide gels. Fluorography (upper panel) and RNA staining (lower panel) are shown.
C. Methylation of the 30S ribosomal subunit by GidB. The 30S and 50S ribosomal subunits from the Δ*gidB* strain were used as the substrates. Values are means ± SD..
D. Determination of the methylated nucleotide by 2D-TLC. Radiolabelled nucleotides were detected using fluorography. Dotted circles show the migration of the four canonical nucleotides used as UV markers.
E. *E. coli* Δ*gidB* strain lacks m^7G modification in 16S rRNA. 16S rRNAs from the wild-type (upper panel) and Δ*gidB* (lower panel) strains were isolated, digested completely to nucleosides and analysed by HPLC. The peaks for m^7G, m^5C, m^2G and m^3U are indicated by arrows.

 Molecular Microbiology, **63**, 1096–1106

forming an *in vitro* methylation reaction using the 30S and 50S subunits instead of the intact 70S ribosome. We found that most of the radioactivity was incorporated into the 30S subunit (Fig. 4C), which includes the 16S rRNA. GidB was unable to methylate naked 16S rRNA (data not shown), implying that the enzyme requires 16S rRNA to be properly folded for efficient reaction.

GidB target is G527 of 16S rRNA

There are 10 known methylatable nucleosides within the *E. coli* 16S rRNA (Andersen and Douthwaite, 2006): $m^6{}_2A$ (*N*6-dimethyladenosine at positions 1518 and 1519), m^4Cm (*N*4, $O^{2'}$-dimethylcytidine at position 1402), m^5C (5-methylcytidine at positions 967 and 1407), m^2G (2-methylguanosine at positions 966, 1207 and 1516), m^7G (7-methylguanosine at position 527) and m^3U (3-methyluridine at position 1498). In addition, the genes responsible for methylating $m^6{}_2A1518$, 1519 (*rsmA* = *ksgA*), m^5C967 (*rsmB* = *fmu*), m^5C1407 (*rsmF* = *yebU*), m^2G1207 (*rsmC* = *yjjT*) and m^3U1498 (*rsmE* = *yggJ*) are well documented (Andersen and Douthwaite, 2006). We therefore postulated that *gidB* is involved in the methylation of $m^4Cm1402$, m^2G966, m^2G1516 or m^7G527, and that *gidB* mutants should fail to methylate one or more of those residues. To test this, we identified the methylated nucleosides using two-dimensional thin-layer chromatography (2D-TLC). Following *in vitro* methylation of the 30S ribosomal subunits using purified GidB and [*methyl*-^{3}H]SAM, the ^{3}H-labelled 16S rRNA was recovered and completely hydrolysed into 5′-monophosphate nucleosides using nuclease P1, and the hydrolysate was subjected to 2D-TLC followed by fluorography. We found that the migration characteristics of the radiolabelled compound were identical to those of m^7G 5′-monophosphate (Fig. 4D). Because *E. coli* 16S rRNA has only one m^7G residue (Andersen and Douthwaite, 2006), it is apparent that GidB catalyses the methylation of G527.

The formation of m^7G by GidB was further confirmed by nucleoside analysis using high-performance liquid chromatography (HPLC) (Fig. 4E). When Δ*gidB* 16S RNAs were digested into nucleosides using nuclease P1 plus alkaline phosphatase and analysed by reverse-phase HPLC, the peak corresponding to m^7G was absent, whereas the peaks for m^5C, m^2G and m^3U were detected at normal intensity as was in wild-type 16S RNA. These results clearly demonstrated that GidB is responsible for the *in vivo* methylation of 16S rRNA apparently at G527. It is noteworthy that G527 is located within the 530 loop and that this nucleotide interacts directly with streptomycin (Fig. 5) (Carter *et al.*, 2000).

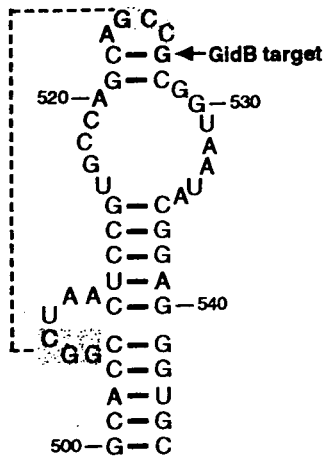

Fig. 5. Secondary structure of the 530 loop region of *E. coli* 16S rRNA. The GidB target site (G527) is indicated by an arrow. Nucleotides known to be involved in the binding of streptomycin are shown in red; those that participate in the formation of the pseudoknot structure are shown in light cyan and connected by a dotted line.

In contrast to most of streptomycin-resistant mutations in *E. coli*, *gidB* mutations did not lead to hyperaccuracy, as determined by a stop codon read-through assays (Table 2), thus suggesting, in turn, that the *gidB*-mutant ribosome has a reduced affinity for streptomycin.

gidB *mutations occur at a high frequency in streptomycin-resistant clinical isolates of* M. tuberculosis

Given the frequent occurrence of *gidB* mutations in spontaneous *M. tuberculosis* mutants showing low-level resis-

Table 2. Effects of *E. coli gidB* and *rpsL* mutations on read-through of the UAG nonsense codon.

Genotype	*lacZ* allele	β-Galactosidase activity[a] (Miller units)	Frequency of read-through (%)	Relative read-through
Wild type	*lacZ105*(Am)	21.1 ± 1.57	0.57	1
	lacZ$^+$	3680 ± 210		
Δ*gidB*	*lacZ105*(Am)	18.9 ± 1.67	0.49	0.86
	lacZ$^+$	3881 ± 492		
rpsL^{K42T}	*lacZ105*(Am)	0.39 ± 0.18	0.013	0.02
	lacZ$^+$	2892 ± 219		

a. Mean ± SD from four independent experiments.

Table 3. Overall profile for mutations within the *gidB*, *rpsL* and *rrs* genes from *M. tuberculosis* clinical isolates.

Sample group	Streptomycin susceptibility[a]	Number of strains sequenced	Number of mutants						
			gidB	*rpsL*	*rrs*	*gidB rpsL*	*gidB rrs*	*gidB rpsL rrs*	None
I	R (20 μg ml^{-1})	42	13	19	1	6	2	1	0
	S (20 μg ml^{-1})	54	15	0	2	0	1	0	36
II	R (10 μg ml^{-1})	15	6	8	0	0	1	0	0
	S (10 μg ml^{-1})	21	0	0	0	0	0	0	21
Total		132	34	27	3	6	4	1	57

a. Determined on Ogawa egg medium.
R, resistant; S, susceptible.

tant phenotype (Table 1), we suspected that these mutations should be present in a considerable number of streptomycin-resistant clinical isolates. To address this possibility, we examined 132 randomly selected clinical *M. tuberculosis* isolates from Japanese tuberculosis patients, including 57 that were streptomycin-resistant and 75 that were streptomycin-susceptible. The level of resistance to nine antituberculosis antibiotics and the presence or absence of mutations in *gidB*, *rpsL* and *rrs* are summarized in Tables S2 and S3, while the overall mutation profile is summarized briefly in Table 3. The *rrs* mutations, A514C and A1401, were not considered as streptomycin-resistance mutations in Table 3 because the presence of these mutations in clinical isolates susceptible to streptomycin (see Tables S2 and S3) indicates irrelevancy of these mutations to streptomycin resistance [A1401 mutation is reportedly known to confer kanamycin resistance (Suzuki *et al.*, 1998)]. Sample groups I and II represent *M. tuberculosis* strains isolated before and after 2000 respectively. In that year, the standard streptomycin concentration used to discriminate resistance and susceptibility in Japan was changed from 20 μg ml^{-1} to 10 μg ml^{-1}.

As expected, in group II samples, *gidB* mutations were tightly associated with the streptomycin-resistant phenotype, while no mutations were found in streptomycin-susceptible strains ($P = 0.003$, Fisher's exact test). In group I samples, however, which were clustered using 20 μg ml^{-1} streptomycin, *gidB* mutations were found in both streptomycin-resistant and -susceptible fractions, indicating that the MICs for *M. tuberculosis gidB* mutants were higher than 10 μg ml^{-1}, most probably around 20 μg ml^{-1} in the Ogawa egg medium used for drug susceptibility testing. The low-level streptomycin-resistance phenotype of *M. tuberculosis gidB* mutants was confirmed by streaking several representatives onto Middlebrook 7H11 agar medium containing streptomycin (Table S3). Notably, *gidB* mutations were found at a high frequency of 33% (19/57) among isolates classified to resistant strain. The frequency of *gidB* mutations was comparable to that of *rpsL* mutations (47%; 27/57), and even double (*gidB rpsL* and *gidB rrs*) and triple (*gidB rpsL rrs*) mutations were detected at a frequency of 18% (10/57), indicative of the importance of *gidB* mutations to the development of high-level resistance (see below). Moreover, the *gidB rpsL* double mutants displayed a variety of *rpsL* mutations, including T35N, R86P, K88Q and K88T mutations (Table S2), that are found only rarely in high-level streptomycin-resistant clinical isolates (Böttger *et al.*, 1998).

The majority of the clinical isolates (70%; 93/132) had an amino acid substitution at codon 92 (Glu to Asp; E92D) of *gidB*. Glu-92 is thought to be the ancestral type, because this residue is conserved without exception in high G+C Gram-positive bacteria. However, examination of several mutant D92 strains and wild-type E92 strains showed that this substitution did not account for the difference in sensitivity to streptomycin (Table S3). Consequently, we do not consider this alteration to be a streptomycin-resistance mutation.

gidB *mutations result in vigorous emergence of high-level streptomycin-resistant mutants*

The results described above led us to hypothesize that cells may be more likely to acquire high-level streptomycin resistance if they carry a *gidB* mutation in their genetic background. This was tested by comparing the frequencies at which high-level streptomycin-resistant mutants emerge from wild-type and *gidB* mutant strains on plates containing a high concentration of streptomycin. In wild-type *E. coli*, the frequency at which high-level streptomycin-resistant mutants emerged was 1.1×10^{-9}, but the frequency was substantially higher (by 450-fold) in the *gidB* mutant (Table 4), always accompanied by an *rpsL* mutation (data not shown). This was also true for *M. smegmatis*, although the increase was only 11-fold. The results obtained with three *M. tuberculosis* strains carrying *gidB* mutations were remarkable. High-level streptomycin-resistant mutants (often accompanied by an *rpsL* mutation) emerged at an extraordinary frequency of 10^{-4}, which represents > 2000-fold increase over the frequency of their emergence from wild-type strains ($< 3 \times 10^{-8}$). In contrast, virtually no difference was

Table 4. Effect of *gidB* mutation on emergence of high-level streptomycin-resistant mutants.[a]

Strain	Streptomycin (μg ml^{-1}) used for high-level resistance	Frequency of mutants	Relative frequency
E. coli	50		
Wild type		1.1×10^{-9}	1
gidB mutant		5.0×10^{-7}	450
M. smegmatis	100		
Wild type		6.3×10^{-9}	1
gidB mutant		6.8×10^{-8}	11
M. tuberculosis	16		
Wild type			
No. 05-028		$< 5.4 \times 10^{-8}$	1
No. 05-048		$< 3.1 \times 10^{-8}$	1
gidB mutant			
No. 05-029		1.7×10^{-4}	> 2000
No. 04-034		1.4×10^{-4}	> 2000
No. 03-075		1.2×10^{-4}	> 2000

a. Selected on LB (for *E. coli*), R (for *M. smegmatis*) or 7H11 (for *M. tuberculosis*) agar.

detected, as examined and compared between *M. smegmatis gidB* and wild-type strains, in the frequency of emergence of mutants resistant to antituberculosis drugs other than streptomycin (we tested kanamycin, rifampicin, ethambutol and isoniazid) (data not shown). These results indicate that the *gidB* mutations do not affect the overall mutation rate of cells.

Discussion

The bacterial ribosome is a major target for antibiotics (Poehlsgaard and Douthwaite, 2005). The aminoglycoside antibiotic streptomycin, the first antibiotic found to target the ribosome, has been important in the treatment of tuberculosis. In addition, streptomycin serves as an essential molecular probe to dissect 'decoding' process of protein synthesis (Ogle and Ramakrishnan, 2005). Recent publications of the crystal structures of the 30S and 50S ribosomal subunits (Ban *et al.*, 2000; Carter *et al.*, 2000; Wimberly *et al.*, 2000), as well as the intact 70S ribosome (Korostelev *et al.*, 2006; Selmer *et al.*, 2006), have increased our understanding of the mechanism of protein synthesis and the actions of antibiotics. The A site of the 30S subunit consists of a pocket formed by the so-called 530 loop, a portion of the long helix 44, and helix 34 in the 16S rRNA (Wimberly *et al.*, 2000). The only protein locating in the vicinity of the A site is the S12 ribosomal protein. Streptomycin binds to the phosphate backbone of 16S rRNA in four different domains – U14 in helix 1, G526 and G527 in the 530 loop, A913 and A914 in helix 27/28, and C1490 and G1491 in helix 44 – through it also forms both salt bridges and hydrogen bonds and makes contact with the S12 protein (Carter *et al.*, 2000). Thus, streptomycin perturbs the A site function, eventually leading to misreading of the genetic code during translation (Ogle and Ramakrishnan, 2005). The 530 loop region is one of the most highly conserved features of 16S rRNA and appears to play a key role in mediating the accuracy of protein synthesis (Powers and Noller, 1991; Wimberly *et al.*, 2000; Ogle and Ramakrishnan, 2005). Mutations in this region often result in resistance to streptomycin (Melancon *et al.*, 1988; Powers and Noller, 1991; Springer *et al.*, 2001). However, no mutations had ever been found in the invariant nucleotide G527. Consequently, our conclusion that failure to methylate G527 results in resistance to streptomycin is striking, although methylation at position G527 was not actually demonstrated in the present work.

The present work, however, demonstrated unambiguously that loss of the m^7G modification in 16S rRNA due to *gidB* mutations results in resistance to streptomycin. This was somewhat unusual, given that resistance to most drugs that interact with ribosomes is associated with changes in the rRNA sequence (Springer *et al.*, 2001), acquisition of methylated bases (Cundliffe, 1989; Douthwaite *et al.*, 2005) or alteration of ribosomal proteins (Poehlsgaard and Douthwaite, 2005). Our findings are not unprecedented, however. Resistance to kasugamycin, another aminoglycoside antibiotic, results from the loss of a methylase, RsmA (also known as KsgA), which methylates bases 1518 and 1519 of the *E. coli* 16S rRNA (Helser *et al.*, 1972). Likewise, resistance to capreomycin, a cyclic peptide antibiotic used as a second-line antituberculosis drug, was recently shown to result from loss of another methylase, 2′-O-methyltransferase (encoded by *tlyA*), which methylates the pentose moieties of nucleotides 1409 of 16S rRNA, 1920 of 23S rRNA (Johansen *et al.*, 2006). Thus, acquisition of drug resistance from a lack of rRNA methylation appears to be fairly common among bacteria, although unlike *gidB*, *tlyA* homologues are found only in limited number of bacteria. As we have now established that GidB is an rRNA methyltransferase, we propose that *rsmG* (rRNA small subunit methyltransferase gene G) would be a more appropriate designation than *gidB*, based on James Ofengand's nomenclature system for rRNA modifying enzymes (Andersen and Douthwaite, 2006). (Nonetheless, to avoid confusion, we have used the gene name *gidB* through this paper.)

Homologues of *gidB* are highly conserved among eubacteria, so it was somewhat surprising that, despite the apparently important contribution made by GidB to ribosomal function, disruption of *gidB* had no effect on the growth of *E. coli* (Fig. 1C) or *M. smegmatis* (Y. Tanaka, S. Okamoto and K. Ochi, unpublished). In addition, high-level resistance to streptomycin in *M. tuberculosis* is predominantly linked to mutations in *rpsL* which do not carry a fitness cost (Böttger *et al.*, 1998; Sander *et al.*, 2002). Therefore, it is apparent that two major resistance mecha-

Table 5. Bacterial strains used in this study.

Strain	Description	Source[a]
E. coli		
BW25113	*Δ(araD-araB)567 ΔlacZ4787*(::rrnB-3) *lacIp-4000*(lacI^q) λ$^-$ *rph-1 Δ(rhaD-rhaB)568 hsdR514*	CGSC
JWK3718	BW25113 *ΔgidB::kan*	NBRP
CAG12080	MG1655 *zah-281::*Tn*10*	NBRP
DEV6	*lacZ105*(Am) λ$^-$ *galU65 relA1 spoT1 thi-1*	CGSC
SEC166	DEV6 *zah-281::*Tn*10*	This study
SEC167	DEV6 *zah-281::*Tn*10 lacZ*$^+$	This study
SEC170	DEV6 *ΔgidB::kan zah-281::*Tn*10*	This study
SEC171	DEV6 *ΔgidB::kan zah-281::*Tn*10 lacZ*$^+$	This study
SEC174	DEV6 *rpsL*^{K42T} *zah-281::*Tn*10*	This study
SEC175	DEV6 *rpsL*^{K42T} *zah-281::*Tn*10 lacZ*$^+$	This study
W3110	F$^-$ λ$^-$ *rph-1 Inv (rrnD-rrnE)*	Laboratory stock
448T	W3110 *gidB* (frameshift)	This study
S. aureus		
209P	Prototroph, avirulent strain	JCM
M. smegmatis		
5866^T	Type strain, prototroph	JCM
205C	5866^T*gidB* (frameshift)	This study
M. tuberculosis		
05-028	Streptomycin-susceptible strain	Clinical isolate
05-048	Streptomycin-susceptible strain	Clinical isolate
03-075	*gidB* mutant with low-level streptomycin resistance	Clinical isolate
04-034	*gidB* mutant with low-level streptomycin resistance	Clinical isolate
05-029	*gidB* mutant with low-level streptomycin resistance	Clinical isolate

a. NBRP, National BioResource Project (NIG, Japan): *E. coli*; CGSC, *E. coli* Genetic Stock Centre; JCM, Japan Collection of Microorganisms.

nisms (due to *gidB* or *rpsL* mutation) observed in strains isolated from clinical cases (Table 3) do not affect cell's fitness and thus their virulence (i.e. no reduction in virulence).

Most importantly, *gidB* mutants arose spontaneously and at high frequency (10^{-4}–10^{-6}) in organisms including *M. tuberculosis* (Table 1). In addition, it is noteworthy that mutants showing high-level streptomycin resistance arose at an extraordinarily high frequency among cells that carried a *gidB* mutation in their genetic background. This was especially pronounced in *M. tuberculosis*, in which *gidB* mutation caused a > 2000-fold increase in the emergence of mutants with high-level streptomycin resistance (Table 4). Indeed, *gidB rpsL* and *gidB rrs* double mutants, together even with a *gidB rpsL rrs* triple mutant, are frequently detected in clinical isolates from tuberculosis patients (Table 3). As *gidB* mutation did not affect the frequency at which mutants resistant to antibiotics other than streptomycin emerged, it is not likely that GidB functions as an anti-mutator-like protein. Nonetheless, the emergence of high-level streptomycin-resistant mutants at an extraordinary high frequency due to *gidB* mutation is of considerable importance in the treatment of tuberculosis. Although clinical trials have shown the efficacy of streptomycin in the initial phase of tuberculosis treatment, the increasing frequency of resistance to streptomycin at global level has made this drug less useful. Our findings account for this clinical aspect.

Streptomyces coelicolor strain KO-179 with a mutation (*str-19*) conferring low-level streptomycin resistance exhibits an enhanced expression of SAM synthetase, eventually leading to overproduction of antibiotic (Okamoto *et al.*, 2003). As will be reported elsewhere, we have confirmed that *str-19* is a mutation within *gidB* and that a *gidB* knockout mutant constructed by gene manipulation displays similar phenotype as the mutant KO-179, accompanied by an increased protein synthesis activity at late growth phase (K. Nishimura, T. Hosaka, S. Tokuyama, S. Okamoto and K. Ochi, submitted). Although we do not know whether *M. tuberculosis gidB* mutants exhibit an enhanced expression of SAM synthetase and an increased protein synthesis activity as did the *S. coelicolor gidB* mutants, these findings may be helpful in considering the plausible physiological effects of *gidB* mutation in *M. tuberculosis*.

In conclusion, we have identified the mutation conferring low-level resistance to streptomycin that has remained obscure for long time and uncovered the resistance mechanism. Further studies will establish the precise function of GidB in the bacterial ribosome and unravel the molecular mechanisms underlying the vigorous emergence of high-level resistance to streptomycin in *M. tuberculosis*, and perhaps in other pathogenic bacteria.

Experimental procedures

Bacterial strains and culture conditions

The bacterial strains used in this study are listed in Table 5. Unless stated otherwise, *E. coli* BW25113 and an isogenic *ΔgidB::kan* strain JWK3718 were used as the wild-type and *ΔgidB* strains respectively (Baba *et al.*, 2006). *E. coli* and

S. aureus were grown in Luria–Bertani (LB) medium or on LB agar, *M. smegmatis* was grown on R agar, and *M. tuberculosis* was grown on Ogawa egg medium or Middlebrook 7H11 medium. All incubations were done at 37°C.

Generation of spontaneous streptomycin-resistant mutants

Spontaneous low-level streptomycin-resistant mutants (*gidB* mutants) were generated from the wild-type strains of *E. coli* (W3110), *M. smegmatis* (5866^T) and clinical isolates of *M. tuberculosis* (strain no. 05-028 and 05-048). Mutant exhibiting high-level streptomycin resistance (*rpsL* or *rrs* mutants) were obtained from wild-type strains and their respective *gidB* mutants. Portions of a cell suspension of each strain were spread on streptomycin-containing plates. Serial dilutions of the cell suspension were also plated on media without streptomycin to determine the numbers of viable cells in the original cell suspension. When measuring the frequency of resistant mutants, we first conducted single colony isolation, and cells originating from each clone (usually we tested 10–20 clones) were separately examined.

In vitro *translation assay*

Cell-free translation of GFP mRNA was performed as described previously (Hosaka *et al.*, 2006). Aliquots of reaction products were subjected to electrophoresis on 10% native-polyacrylamide gels, and GFP levels were determined using a FluorolImager (Molecular Dynamics).

Plasmid constructions

The *E. coli gidB* gene was amplified using the forward primer, 5′-GGATCCATGCTCAACAAACTCTCCTTACTG-3′, containing a BamHI site, and the reverse primer, 5′-CTGC AGTTAAATTTTATTTGCTTTAATCACCACCAG-3′, containing a PstI site. The gene fragment was amplified using KOD -Plus- DNA polymerase (Toyobo, Japan) and cloned into the pTA2 vector (Toyobo, Japan) using a TArget clone -Plus- TA cloning kit (Toyobo, Japan). After sequence confirmation, the BamHI-PstI fragment was inserted into pQE-80 L (Qiagen), generating the pQE-Eco_gidB. The *gidB* gene from *S. coelicolor* was amplified using the forward primer, 5′-GGATCCATGTCGGAGGCAGCGGAGCT-3′, containing a BamHI site, and the reverse primer, 5′-CTGCAGC TATCCGCGGCGTCGACGCGT-3′, containing a PstI site, and cloned into pQE-80L in analogous fashion, generating the plasmid pQE-Sco_gidB.

Expression and purification of (His)$_6$-GidB protein

Escherichia coli BL21/pLysS cells harbouring pQE-Eco_gidB were grown at 37°C to an OD_{600} of 0.6 in 200 ml of LB medium containing 0.2% glucose, 50 μg ml^{-1} carbenicillin and 25 μg ml^{-1} chloramphenicol. Expression was induced with 1 mM isopropyl-β-D-thiogalactopyranoside, and incubation was continued at 37°C for an additional 4 h. Cells were harvested by centrifugation and frozen at −70°C. The cell pellet was resuspended in 16 ml of binding buffer [20 mM sodium phosphate (pH 7.4), 500 mM NaCl, 50 mM imidazole, 3 mM dithiothreitol] containing Complete™ protease inhibitor cocktail (Rosche) and sonicated. Insoluble material was removed by centrifugation, and the crude extract was chromatographed on a 1 ml HisTrap HP column (GE Healthcare Bio-Sciences) equilibrated in binding buffer. The (His)$_6$-GidB protein was eluted with a linear gradient of 50–300 mM imidazole in binding buffer. The fractions containing (His)$_6$-GidB were pooled, dialysed against storage buffer [20 mM HEPES-KOH (pH 7.5), 100 mM KCl, 3 mM dithiothreitol, 20% (v/v) glycerol], concentrated and stored at −70°C until use.

In vitro *methylation assay*

Methylation reactions were performed using 20 pmol of 70S ribosomes, 30S subunits, 50S subunits or 16S rRNA as substrates in 20 μl of 50 mM HEPES-KOH (pH 7.5), 100 mM NH_4Cl, 2 mM $Mg(OAc)_2$, 5 mM dithiothreitol, and 10% (v/v) glycerol containing 4–100 pmol of (His)$_6$-GidB as the methylase. The methyl donor [*methyl*-^{3}H]SAM (15 Ci mmol^{-1}; GE Healthcare Bio-Sciences) was added to a final concentration of 3 μM, and the mixtures were incubated at 37°C for the indicated times (usually 1–6 h). The reactions were terminated by precipitation with 10% ice-cold trichloroacetic acid for kinetic analyses or by extraction with an ISOGEN reagent (Nippon Gene, Japan) for fluorographic analysis. To measure radioactivity, samples were collected on glass filters (Whatman GF/F), and radioactivity on the filter was measured by scintillation counting. For fluorographic analysis, extracted rRNAs were precipitated with isopropanol, dissolved in TE buffer, and applied onto acrylamide gels.

Identification of in vitro *methylated nucleotide*

In vitro methylation reactions were performed with 30S subunits as described above, and the ^{3}H-labelled RNAs were extracted with ISOGEN, precipitated with isopropanol and digested with nuclease P1 (Yamasa, Japan). The 5′-monophosphate nucleosides thus generated were separated by 2D-TLC on cellulose plates using the solvent system I described previously (Grosjean *et al.*, 2004). Radioactive compounds were detected by fluorography using EN3HANCE spray (PerkinElmer).

Analysis of in vivo *methylation profiles of 16S rRNA*

16S RNAs were extracted from 30S subunits isolated from *E. coli* wild-type and Δ*gidB* strains. A 25 μg aliquot of each extract was digested for 3 h at 37°C with nuclease P1 (3 U) and alkaline phosphatase (0.04 U) in 25 μl of reaction mixture containing 20 mM HEPES-KOH (pH 7.5). The resulting nucleosides were analysed by HPLC using an Inertsil ODS-3 column (250 × 2.1 mm, GL Science, Japan) as described (Ikeuchi *et al.*, 2006).

Stop codon read-through assay β-galactosidase activity was measured according to standard protocols (Miller, 1992), except that all incubations were at 30°C. Read-through frequency is expressed as the activity obtained with the *lacZ105*(Am) strain divided by the activity obtained with the wild-type *lacZ* strain.

